ESI

for

Substitution Pattern on Anthrol Carbaldehydes: Excited State Intramolecular Proton Transfer (ESIPT) with a Lack of Phototautomer Fluorescence

Sermsiri Chaiwongwattana,[†] Đani Škalamera,[‡] Nađa Došlić,[§]* Cornelia Bohne,[ǁ] and Nikola Basarić[‡]*

[†] Institute of Science, Suranaree University of Technology, 30000 Nakhon Ratchasima, Thailand

[‡]Department of Organic Chemistry and Biochemistry, Ruđer Bošković Institute, Bijenička cesta 54, 10 000 Zagreb, Croatia. Fax: + 385 1 4680 195; E-mail: nbasaric@irb.hr

[§] Department of Physical Chemistry, Ruđer Bošković Institute, Bijenička cesta 54, 10000 Zagreb, Croatia. Fax: + 385 1 4680 245; E-mail: nadja.doslic@irb.hr

[ǁ]Department of Chemistry, University of Victoria, Box 1700 STN CSC, Victoria BC, V8W 2Y2, Canada.

Table of contents:

1. Synthetic reaction schemes

Carbaldehyde **1** was synthesized by a known route[1] starting from the commercialy available tetralin. In the first step tetralin reacted with succinanhydride under Friedel-Crafts conditions to give keto-acid **6**,[2] and then, the keto group was reduced in a Clemensen reaction.[3] The tricyclic threecyclic system was obtained in a cyclization with CH_3SO_3H catalyst,[4] where **8** is formed under kinetic control in high yield and purity if the reaction is conducted for a short time. Compound **8** in the presence of a strong base (NaH) gave carbanion which reacted with ethyl formate to give product **9** in 81% yield.[5,6] Finnally, aromatization of the policyclic skeleton was carried out with *in situ* generated trityl cation giving target carbaldehyde **1** in 87% yield (Scheme S1).[2]

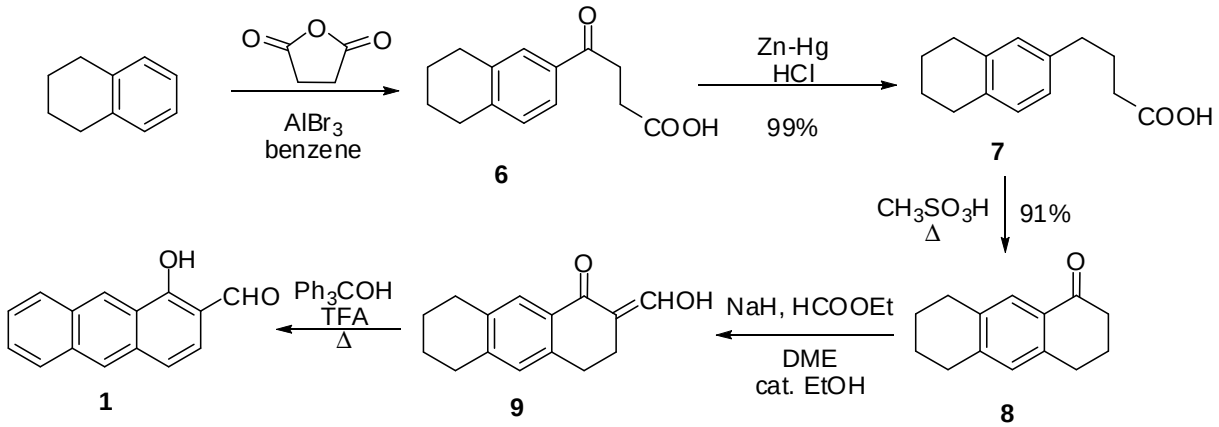

Scheme S1.

Compound **2** was synthesized from 2-anthrol (**10**), prepared by $NaBH_4$ reduction[7] of 2-hydroxyanthraquinone (Scheme S2).[8] In an electrophilic aromatic substitution with dichloromethoxymethane 2-anthrol (**10**) was transformed to a mixture of carbaldehydes **2** and **11**, where the desired carbaldehyde **2** was the main product isolated in 35% yield.

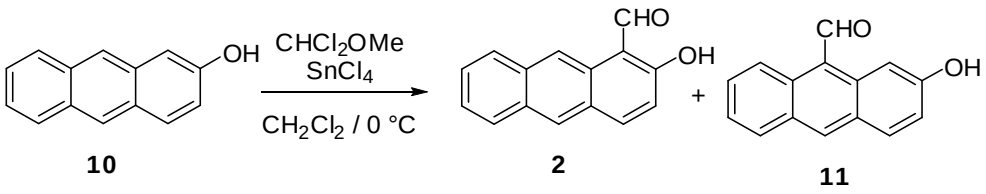

Scheme S2.

Compounds **3**-**5** were prepared from 3-bromo-2-hydroxyanthraquinone (**9**) according to literature precedent.[7] Antraquinone **9** was subjected to a reduction with $NaBH_4$ in alkaline aqueous solution (1M Na_2CO_3) to yield pure 2-bromo-3-anthrol (**14**). In the next step, **14** was treated with excess of BuLi and the lithiated compound reacted with DMF to afford the corresponding aldehyde **3** (Scheme S3). Treatment of antraquinone **9** with an excess of MeLi or PheLi followed by reduction gave methylated anthrol derivative **13-Me** or phenyl derivative **13-Ph**. Compounds **13** in a reaction with BuLi and quenching with DMF afforded carbaldehydes **4** or **5**.

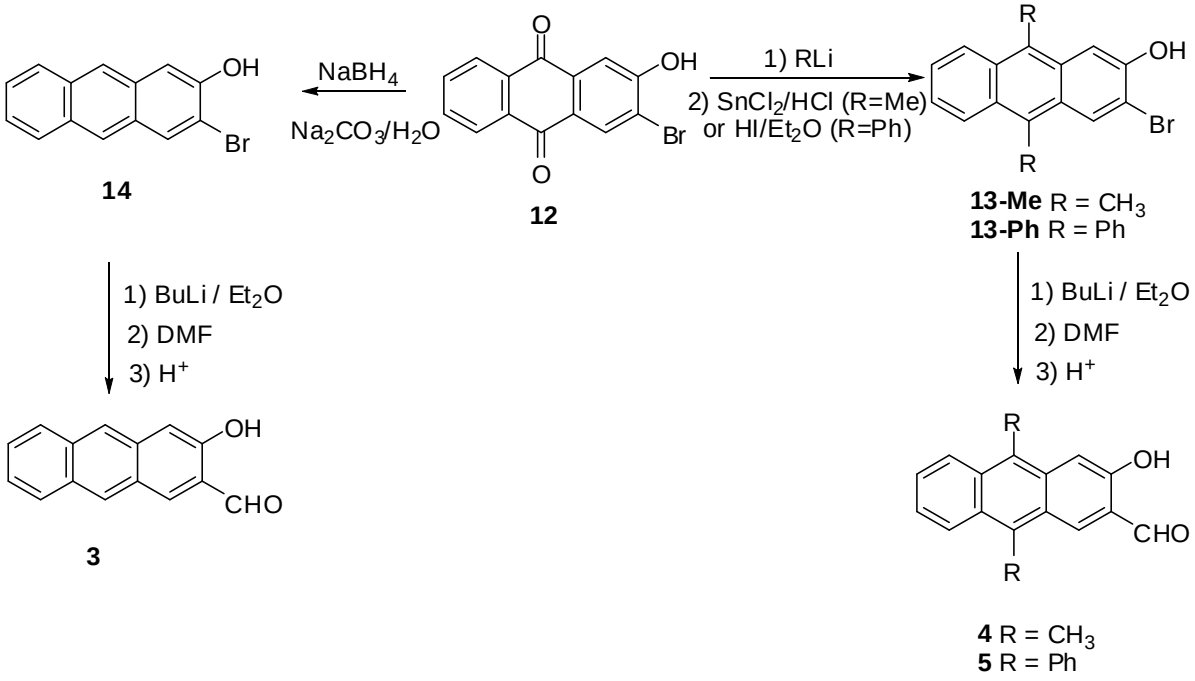

Scheme S3.

2. Calculations

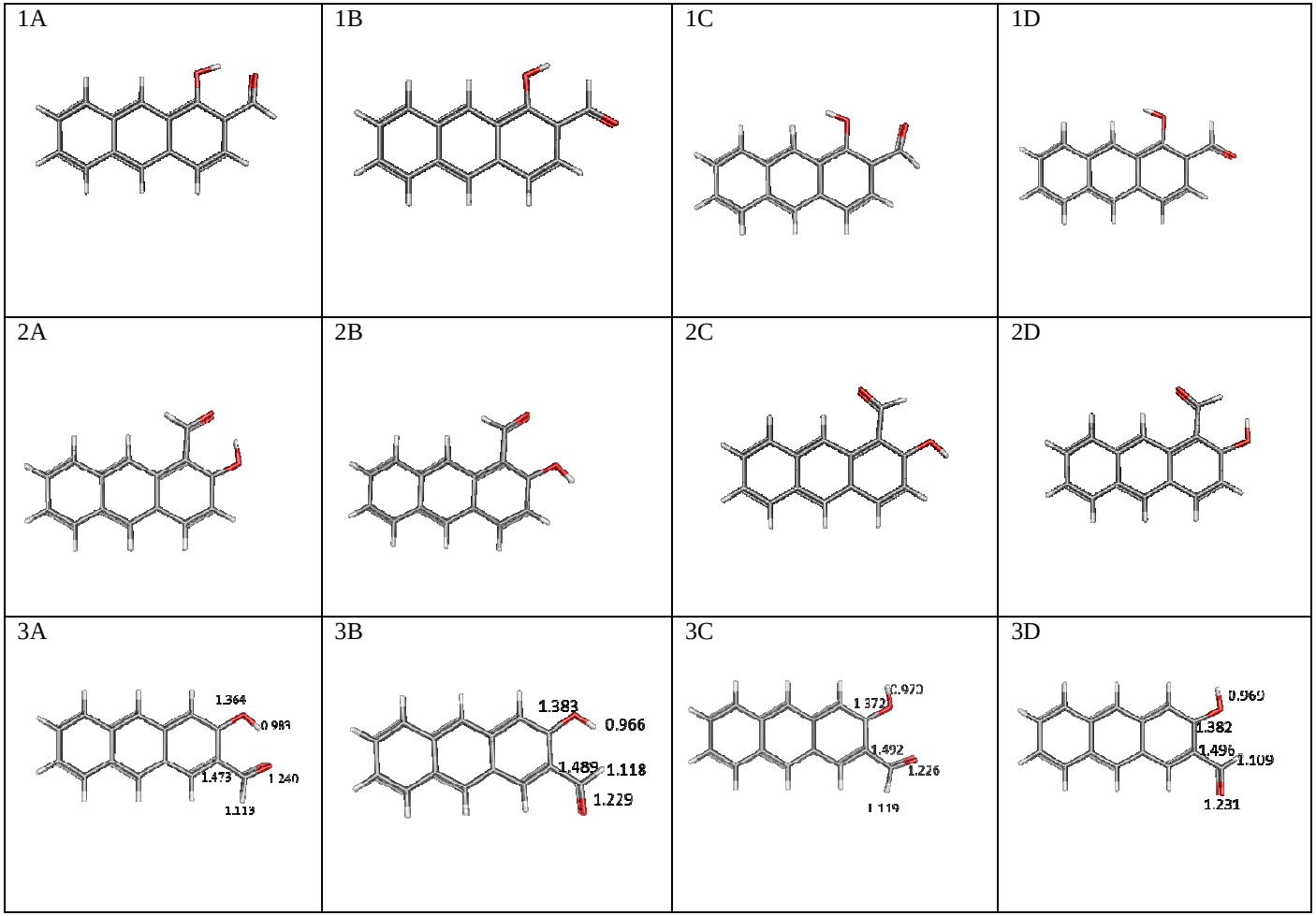

Fig S1. Ground state minimum energy structures of the relevant conformers of **1**-**3**.

Table S1. ADC(2)-/aug-cc-pVDZ energy barriers in eV for conformational changes as obtained from linearly interpolated path between optimized ground (S_0) and excited (S_1) state structures.

Conformational change	S_0 (eV)	S_1 (eV)
2B(S_{0min})→**2D**(S_{0min})	0.28	0.48
3A(S_{0min})→**3B**(S_{0min})	0.66	1.12
3B(S_{0min})→**3D**(S_{0min})	0.16	0.27
3B(S_{1min})→**3D**(S_{1min})	_	0.33
3D(S_{1min})→**3B**(S_{1min})	_	0.09

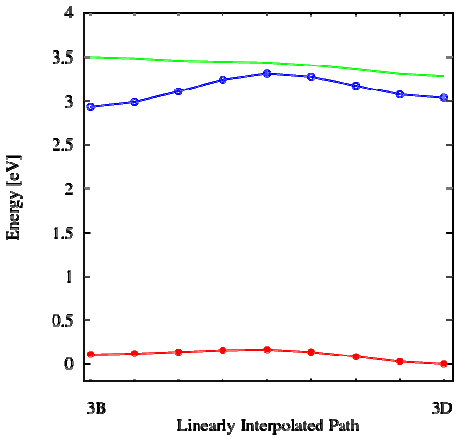

Fig S2. Linearly interpolated path between S_0 (red) optimized structures **3B** and **3D** showing the barriers for the conformational change in the S_0, S_1 (blue) and S_2 (green) states.

Table S2. Vertical excitation energies to the three lowest excited states of **1**, oscillator strengths (in parenthesis) and the most relevant molecular orbitals involved in the excitation. The computations were performed at the ADC(2)/aug-cc-pVDZ level.

	1A		**1B**		**1C**		**1D**	
	ΔE (eV)	MO	ΔE (eV)	MO	ΔE (eV)	MO	ΔE (eV)	MO
S_1	3.07 (0.092)	$L_a(\pi\pi^*)$ H→L	3.21 (0.108)	$L_a(\pi\pi^*)$ H→L	3.17 (0.079)	$L_a(\pi\pi^*)$ H→L	3.24 (0.096)	$L_a(\pi\pi^*)$ H→L
S_2	3.70 (4×10^{-4})	nπ* H-5→L	3.53 (2×10^{-4})	nπ* H-5→L	3.27 (1×10^{-4})	nπ* H-4→L	3.39 (1×10^{-4})	nπ* H-4→L
S_3	3.70 (0.026)	ππ* H-1→L+8	3.72 (0.027)	ππ* H→L+7	3.65 (0.017)	ππ* H→L+8	3.66 (0.025)	ππ* H→L+7

Table S3. Vertical excitation energies to the three lowest excited states of **2**, oscillator strengths (in parenthesis) and the most relevant molecular orbitals involved in the excitation. The computations were performed at the ADC(2)/aug-cc-pVDZ level

	2A		**2B**		**2C**		**2D**	
	ΔE (eV)	MO	ΔE (eV)	MO	ΔE (eV)	MO	ΔE (eV)	MO
S_1	3.17 (0.104)	$L_a(\pi\pi^*)$ H→L	3.19 (0.7×10^{-4})	nπ* H-3→L+1	3.14 (0.113)	$L_a(\pi\pi^*)$ H→L	3.12 (0.106)	$L_a(\pi\pi^*)$ H→L+1
S_2	3.60 (2×10^{-4})	nπ* H-5→L	3.22 (0.098)	$L_a(\pi\pi^*)$ H→L+1	3.34 (2×10^{-4})	nπ* H-5→L	3.19 (2×10^{-4})	nπ* H-4→L+1
S_3	3.77 (0.084)	$L_b(\pi\pi^*)$ H-1→L	3.75 (0.037)	$L_b(\pi\pi^*)$ H-1→L+1	3.70 (0.076)	$L_b(\pi\pi^*)$ H-1→L	3.71 (0.053)	$L_b(\pi\pi^*)$ H-2→L+1

Table S4 Adiabatic excitation energies and vertical emission energies of **1** The computations were performed at the ADC(2)/aug-cc-pVDZ level

	1A	**1B**	**1C**	**1D**
E^a (eV)	2.80	2.98	2.94	3.02
$E^{emission}$ (eV)	2.47	2.71	2.68	2.78

Table S5 Adiabatic excitation energies and vertical emission energies of **2** The computations were performed at the ADC(2)/aug-cc-pVDZ level

	2A	**2B**	**2C**	**2D**
E^{a} (eV)	2.84	2.43	2.41	2.87
$E^{emission}$ (eV)	2.47	1.16	1.26	2.52

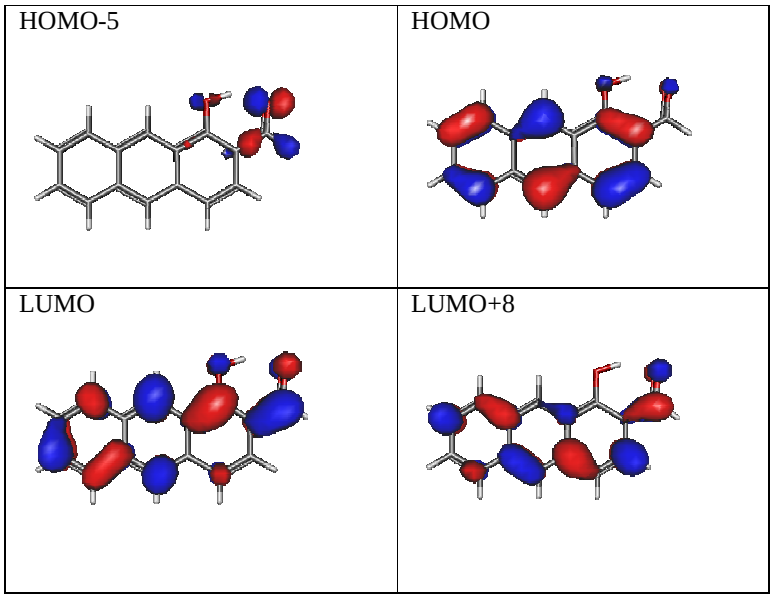

Fig S3. Relevant molecular orbitals contributing to the S_1, S_2 and S_3 transitions of **1A** computed at the geometry of vertical excitation. The computation were performed at the ADC(2)/aug-cc-pVDZ level.

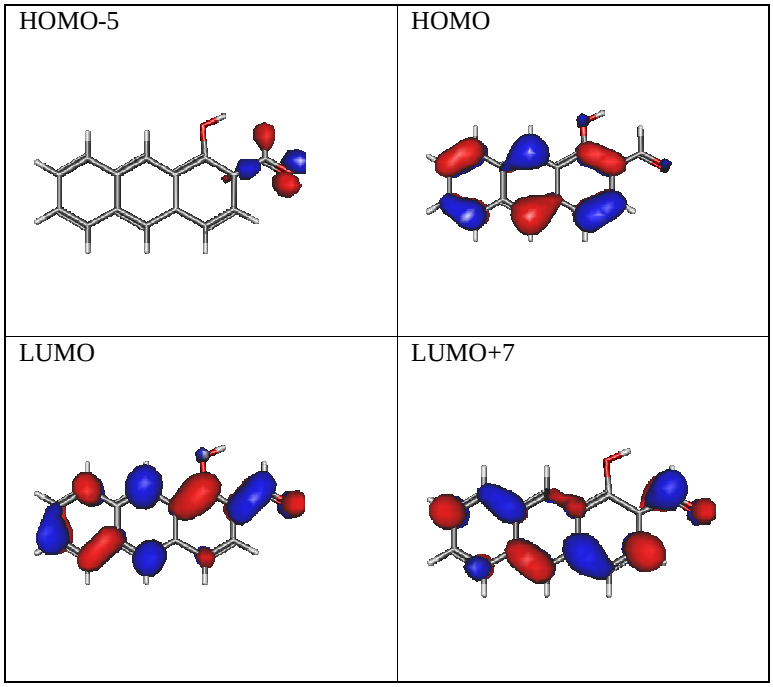

Fig S4. Relevant molecular orbitals contributing to the S_1, S_2 and S_3 transitions of **1B** computed at the geometry of vertical excitation. The computation were performed at the ADC(2)/aug-cc-pVDZ level

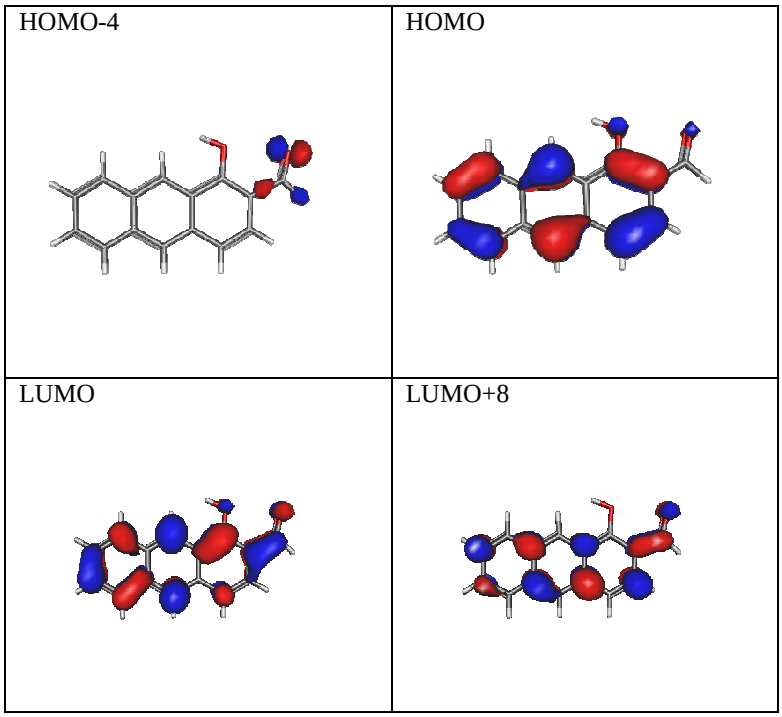

Fig S5. Relevant molecular orbitals contributing to the S_1, S_2 and S_3 transitions of **1C** computed at the geometry of vertical excitation. The computation were performed at the ADC(2)/aug-cc-pVDZ level

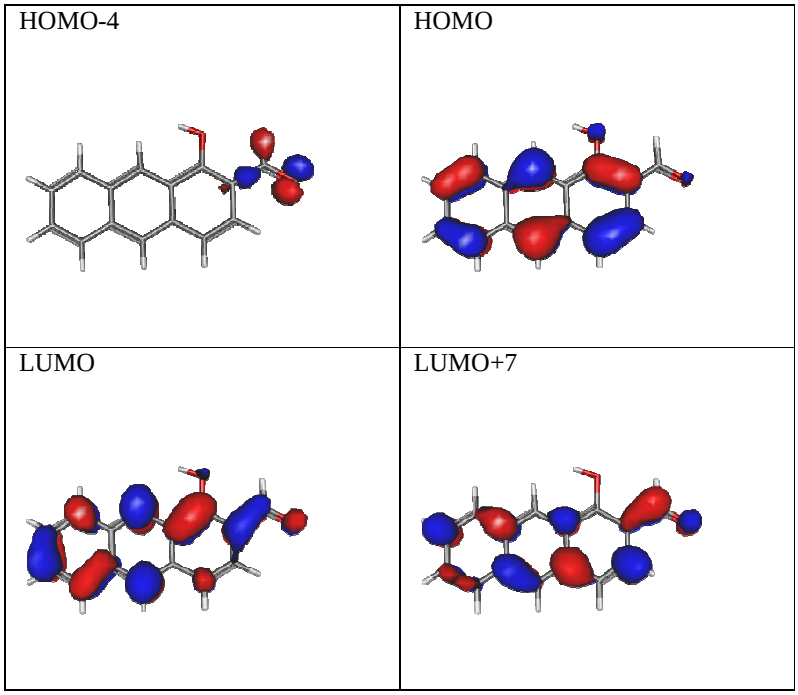

Fig S6. Relevant molecular orbitals contributing to the S_1, S_2 and S_3 transitions of **1D** computed at the geometry of vertical excitation. The computation were performed at the ADC(2)/aug-cc-pVDZ level

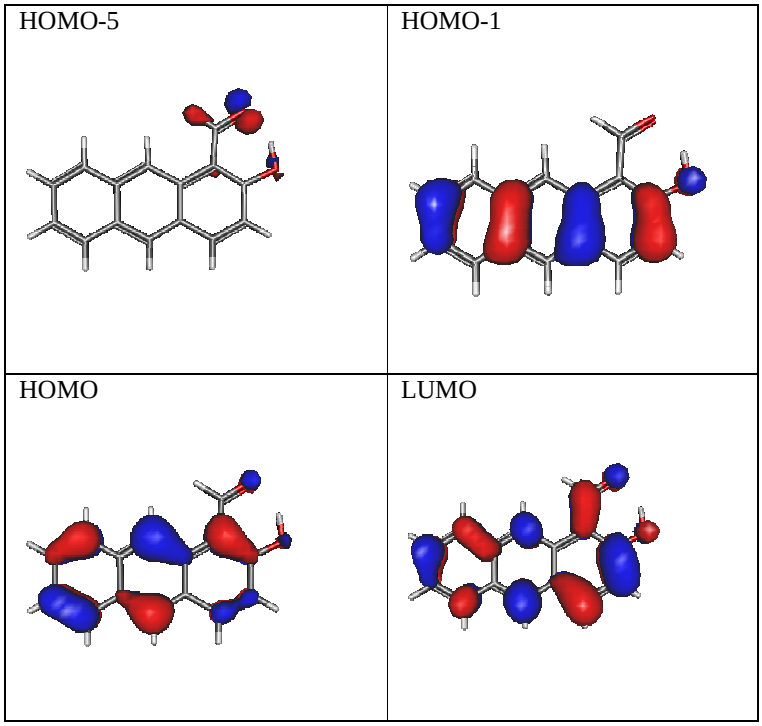

Fig S7. Relevant molecular orbitals contributing to the S_1, S_2 and S_3 transitions of **2A** computed at the geometry of vertical excitation. The computation were performed at the ADC(2)/aug-cc-pVDZ level.

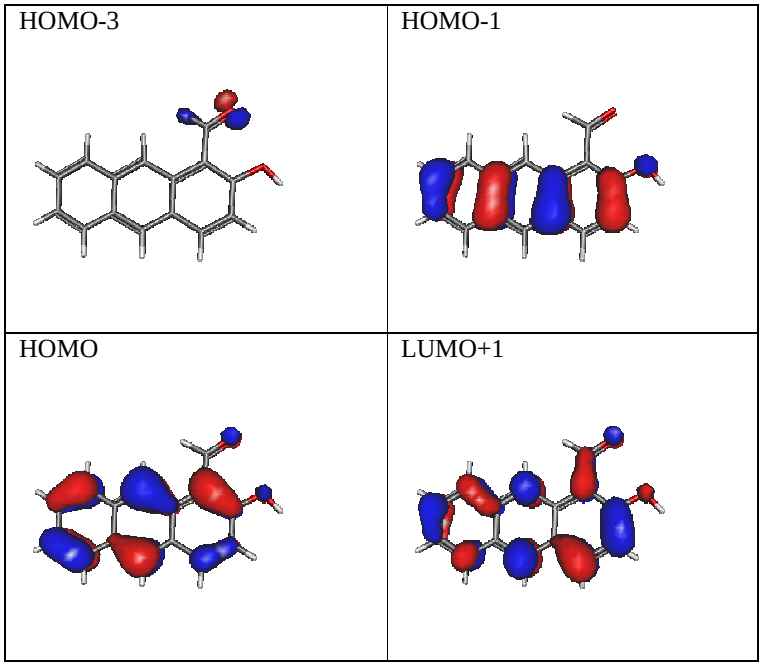

Fig S8. Relevant molecular orbitals contributing to the S_1, S_2 and S_3 transitions of **2B** computed at the geometry of vertical excitation. The computation were performed at the ADC(2)/aug-cc-pVDZ level.

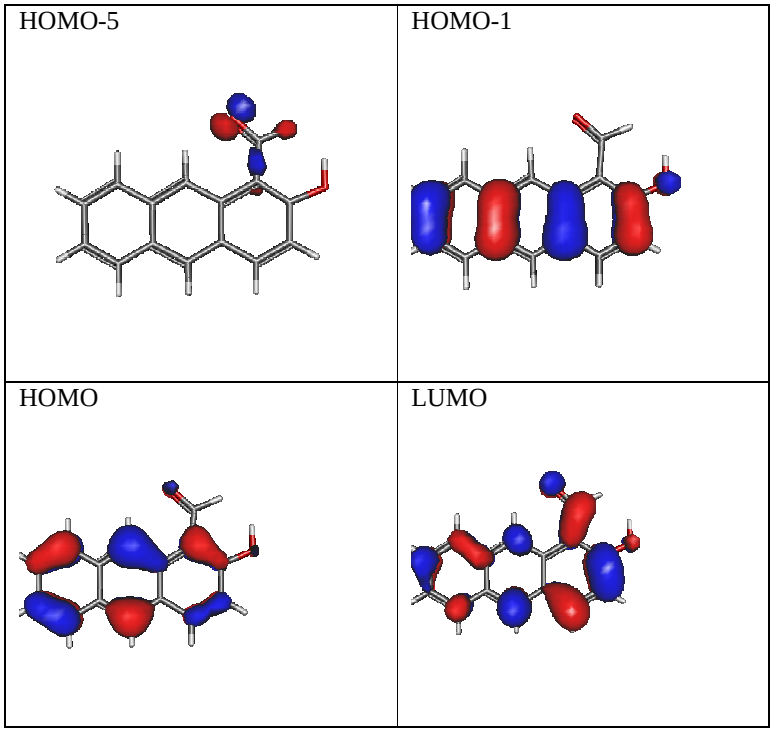

Fig S9. Relevant molecular orbitals contributing to the S_1, S_2 and S_3 transitions of **2C** computed at the geometry of vertical excitation. The computation were performed at the ADC(2)/aug-cc-pVDZ level.

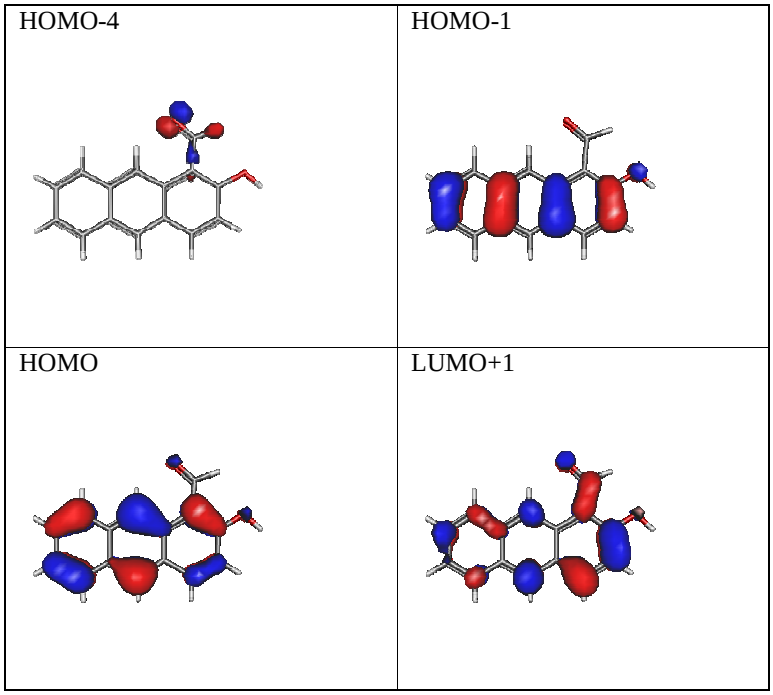

Fig S10. Relevant molecular orbitals contributing to the S_1, S_2 and S_3 transitions of **2D** computed at the geometry of vertical excitation. The computation were performed at the ADC(2)/aug-cc-pVDZ level.

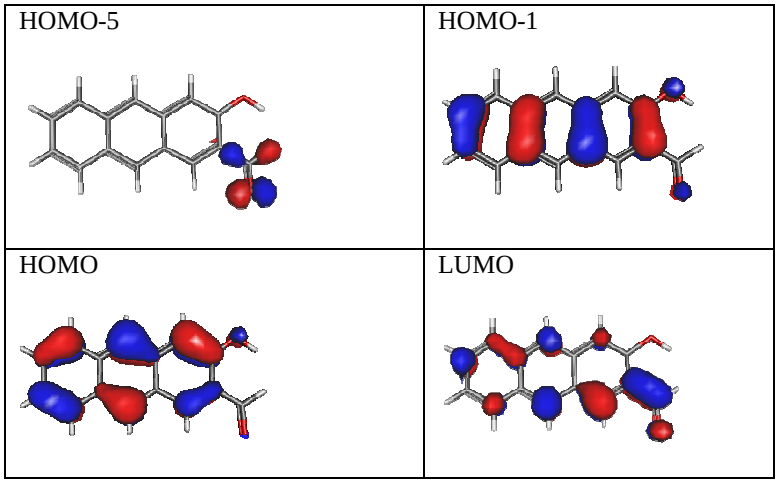

Fig S11. Relevant molecular orbitals contributing to the S_1, S_2 and S_3 transitions of **3B** computed at the geometry of vertical excitation. The computation were performed at the ADC(2)/aug-cc-pVDZ level.

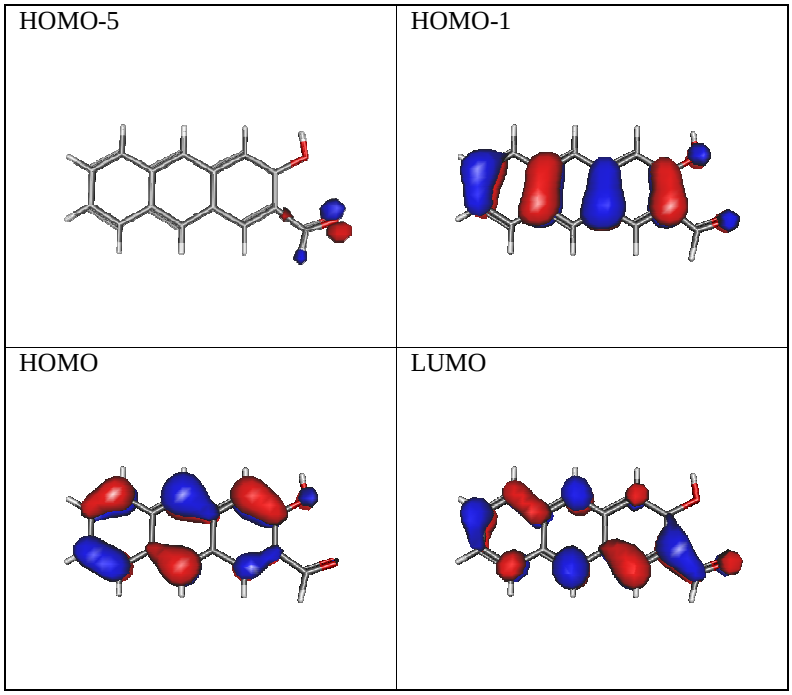

Fig S12. Relevant molecular orbitals contributing to the S_1, S_2 and S_3 transitions of **3C** computed at the geometry of vertical excitation. The computation were performed at the ADC(2)/aug-cc-pVDZ level.

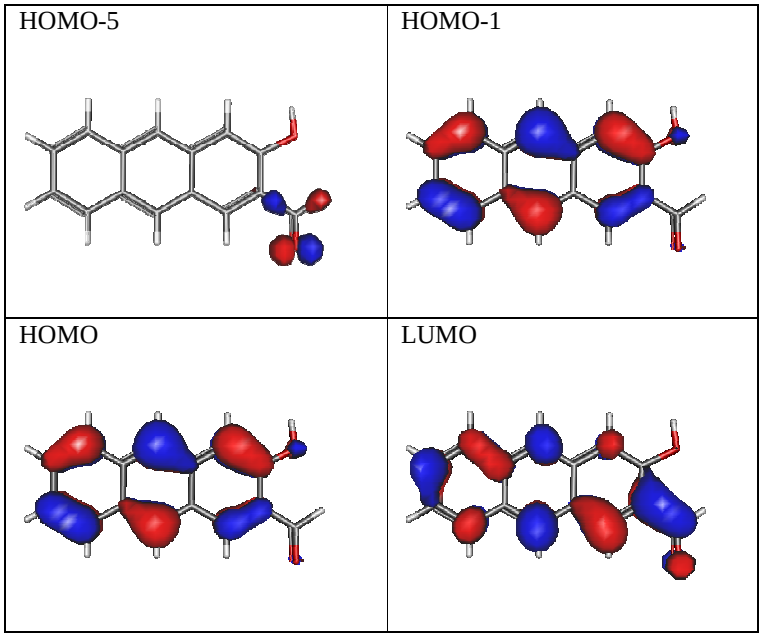

Fig S13. Relevant molecular orbitals contributing to the S_1, S_2 and S_3 transitions of **3D** computed at the geometry of vertical excitation. The computation were performed at the ADC(2)/aug-cc-pVDZ level.

3. UV-vis and fluorescence spectra of 1-5

Table S6. Spectral properties of **1-5**

	Cyclohexane[a] or EtOAc[b]		CH_3CN	
	λ^{a}_{max}/ nm [c]	λ^{em}_{max}/ nm [d]	λ^{a}_{max}/ nm [c]	λ^{em}_{max}/ nm [d]
1	447, 422, 403, 362, 344, 328, 296, 264[a]	460,486, 520	446 (sh), 419, 362, 344, 325, 296, 263	508
2	441, 434, 416, 394, 358, 341, 325, 300, 289, 274, 255[a]	443, 449, 472, 506	432 (sh), 414, 358, 341, 298, 272, 252	506
3	458, 363, 345, 329[a] 452, 362, 344, 328[b]	-[e] 515[b]	449, 362, 344, 327, 274	529
4	-	-	473, 374, 355, 338, 283	565
5	-	-	466, 371, 353, 336, 283	554

[a] Spectra measured in cyclohexane. [b] Spectra measured in EtOAc. [c] Maxima in the absorption spectra. [d] Maxima in the fluorescence spectra. [e] Fluorescence was not detected.

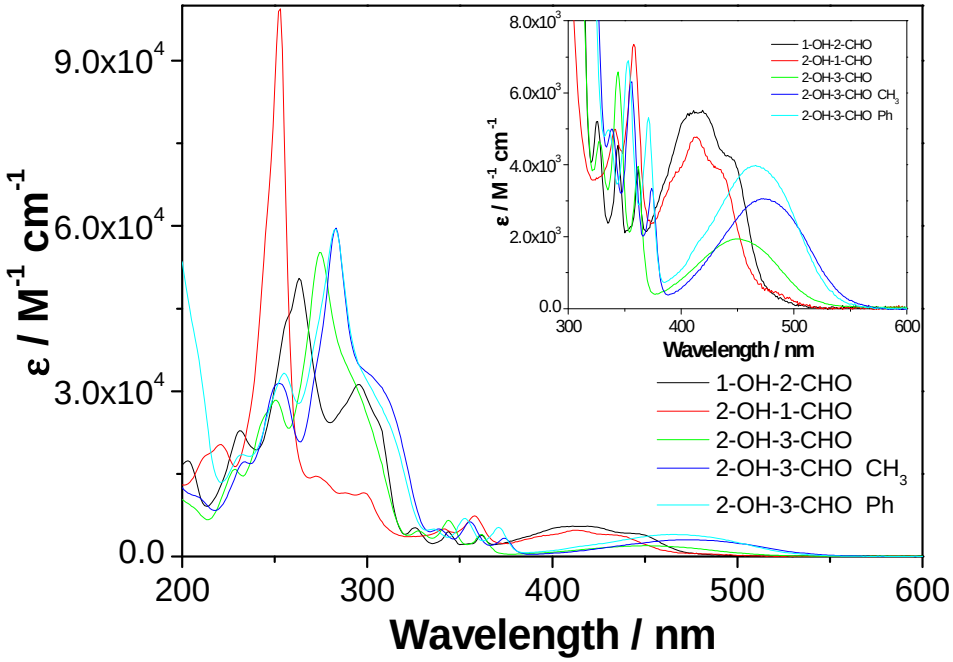

Fig S14. Absorption spectra of **1-5** in CH_3CN.

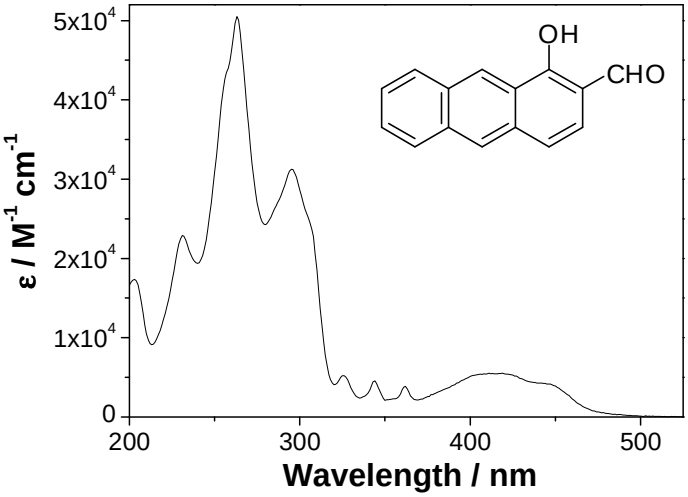

Fig S15. Absorption spectrum of **1** in CH_3CN.

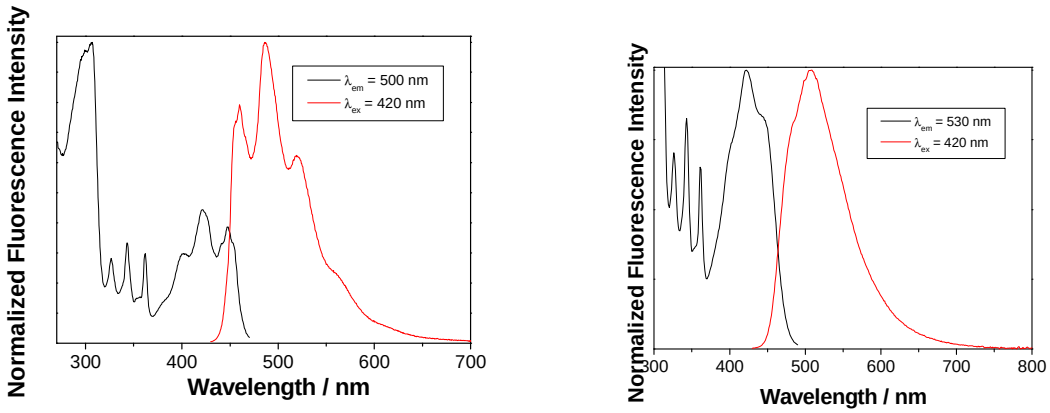

Fig S16. Normalized excitation and emission spectra for **1** in cyclohexane (left) and CH_3CN (right).

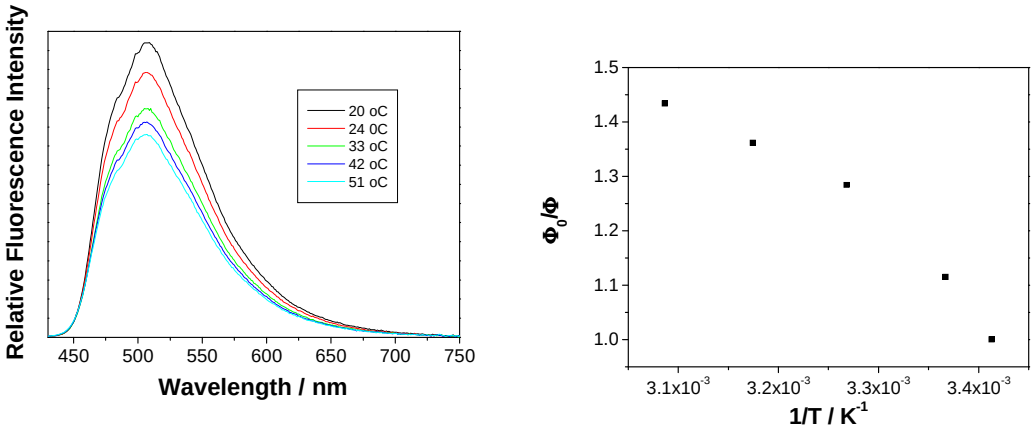

Fig S17. Fluorescence spectra of **1** in CH_3CN (λ_{ex} = 420 nm) at different temperatures.

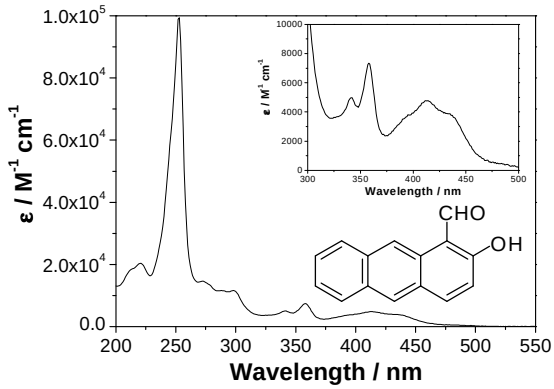

Fig S18. Absorption spectrum of **2** in CH_3CN.

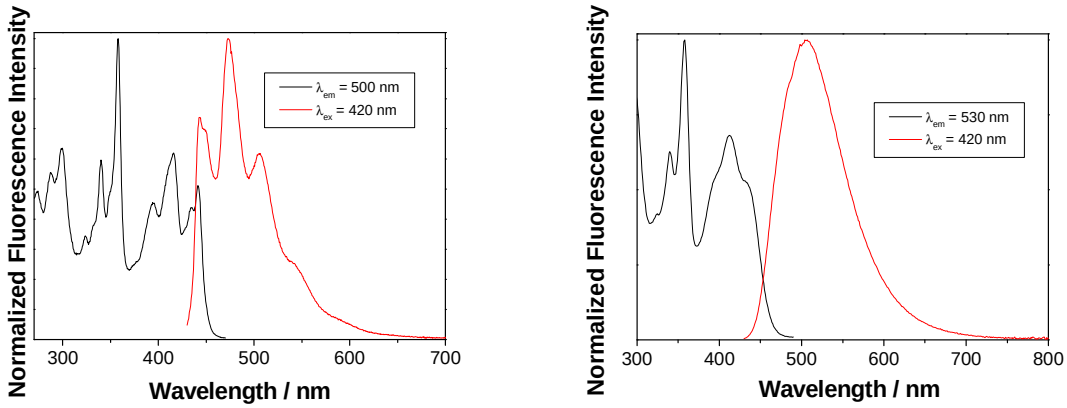

Fig S19. Normalized excitation and emission spectra for **2** right in cyclohexane(left) and CH_3CN (right).

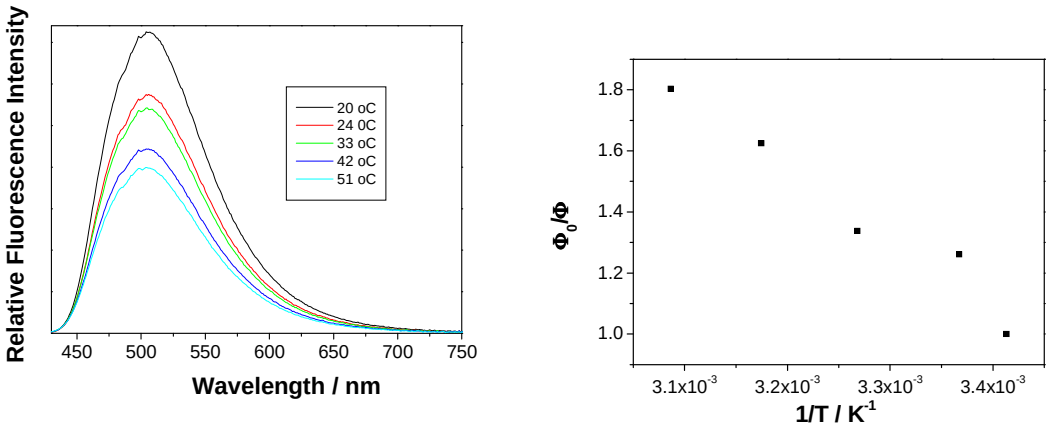

Fig S20. Fluorescence spectra of **2** in CH_3CN (λ_{ex} = 420 nm) at different temperatures.

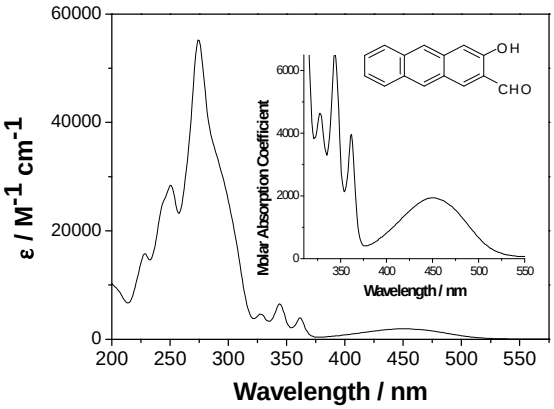

Fig S21. Absorption spectrum of **3** in CH_3CN.

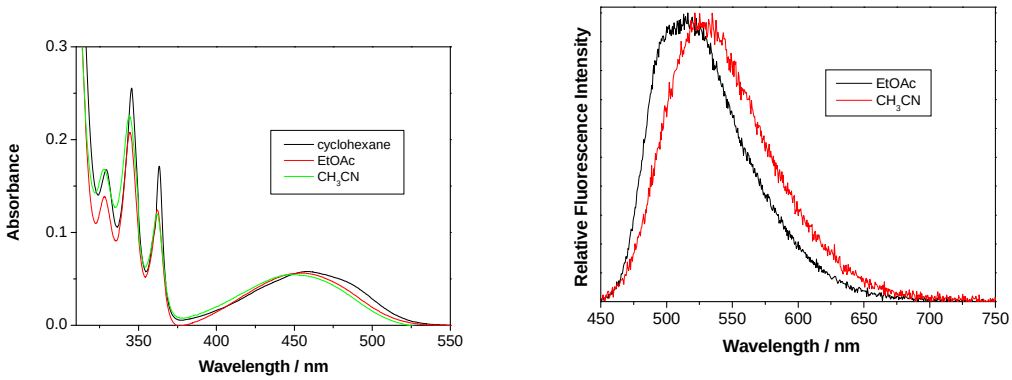

Fig S22. Normalized absorption spectra (left) and emission spectra (right) of **3** in different solvents.

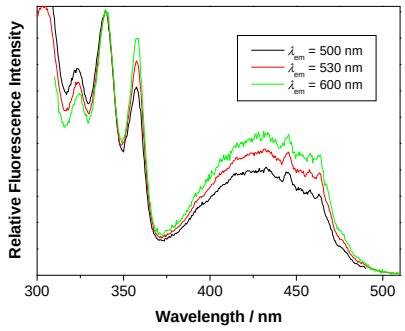

Fig S23. Normalized excitation spectra of **3** in CH_3CN detected at different wavelengths.

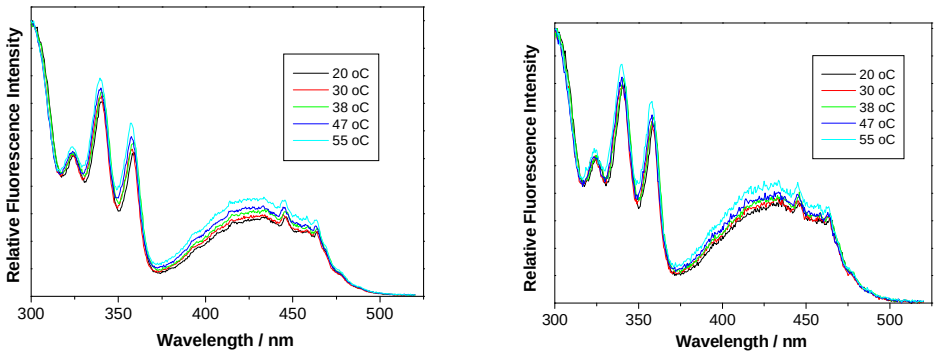

Fig S24. Normalized excitation spectra of **3** taken in CH_3CN at different temperatures by detecting emission at 530 nm (left) or 600 nm (right).

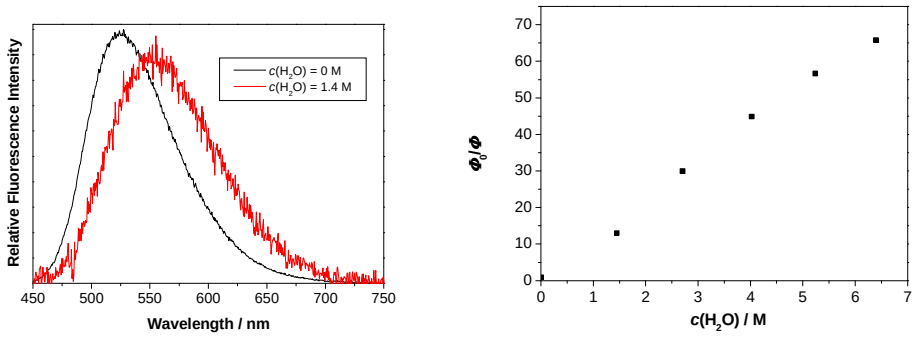

Fig S25. Normalized fluorescence spectra of **3** in CH_3CN at different H_2O concentration (left), and the corresponding Stern-Volmer plot (right).

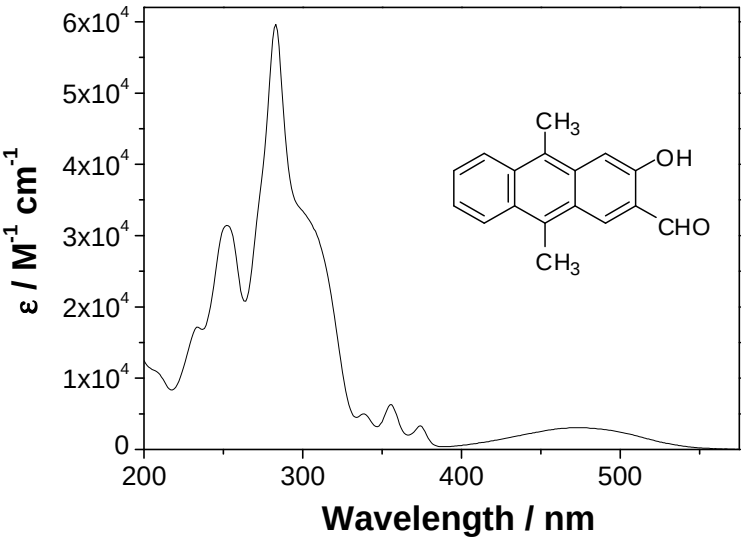

Fig S26. Absorption spectrum of 4 in CH_3CN.

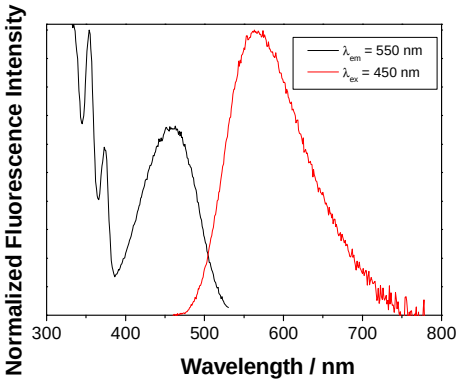

Fig S27. Normalized excitation and emission spectra of **4** in CH_3CN.

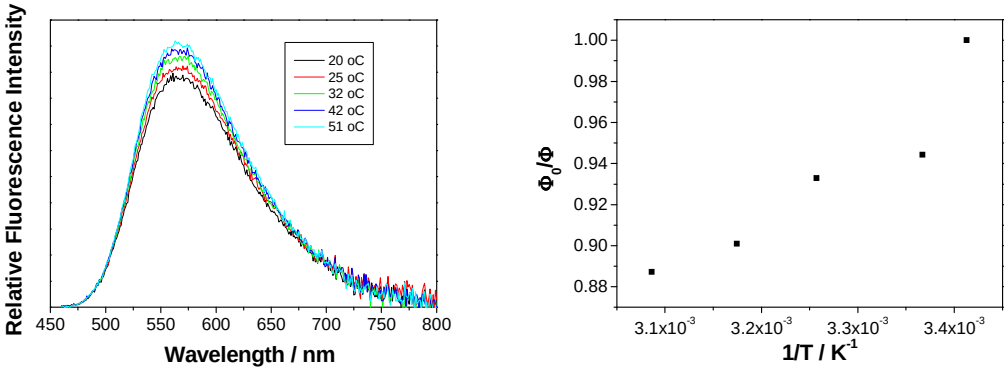

Fig S28. Fluorescence spectra of **4** in CH_3CN (λ_{ex} = 450 nm) at different temperatures.

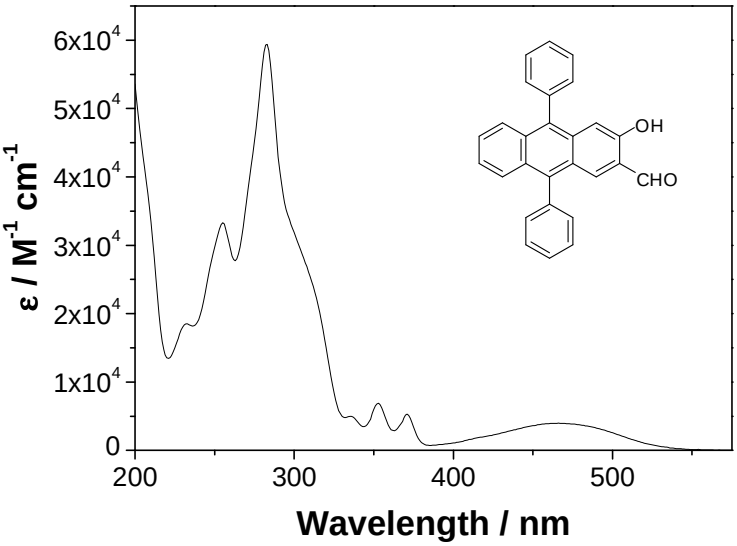

Fig S29. Absorption spectrum of **5** in CH_3CN.

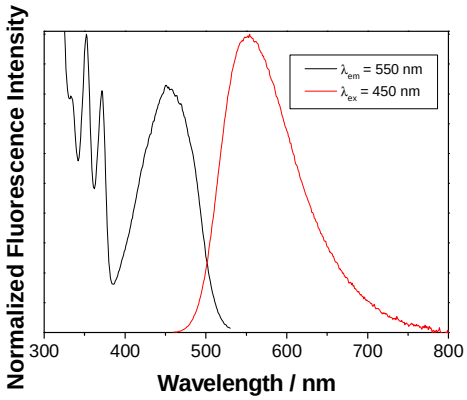

Fig S30. Normalized excitation and emission spectra of **5** in CH_3CN.

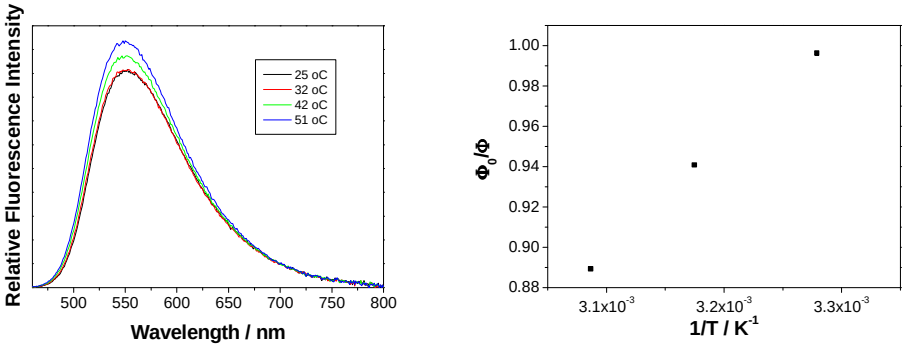

Fig S31. Fluorescence spectra of **5** in CH_3CN (λ_{ex} = 450 nm) at different temperatures.

Table S7. Calculated absorption and emission maxima for **1**-**3** in CH_3CN.

	λ^{a}_{max}/ nm	λ^{a}_{max}/ nm calculated	λ^{em}_{max}/ nm	λ^{em}_{max}/ nm calculated [b]
1	446 (sh), 419	404 (3.07 eV)	508	502 (2.47 eV, **1A**)
2	432 (sh), 414	390 (3.17 eV)	506	502 (2.47 eV, **2A**)
3	449	454 (2.73 eV)	529	541 (2.29 eV, **3B**) 498 (2.49 eV, **3D**)

[a] Lowest energy absorption band. [b] Emissive conformer.

Fluorescence decays, collected over 1023 time channels, were obtained on an Edinburgh Instruments OB920 single photon counter using a pulsed laser diode for excitation at 405 nm. Obtained histograms were fit as sums of exponentials using global Gaussian-weighted non-linear least-squares fitting based on Marquardt-Levenberg minimization implemented in the Fast software package from Edinburgh Instruments. For decays collected at different wavelengths the lifetimes were linked in the global analysis of the fluorescence decays.

Fluorescence decays were fit to a sum of exponentials using the following expression:

$$F\,(t) = \alpha_1 \exp\left(-\frac{t}{\tau_1}\right) + \alpha_2 \exp\left(-\frac{t}{\tau_2}\right) + \alpha_3 \exp\left(-\frac{t}{\tau_3}\right) + \ \ldots \qquad \text{(S1)}$$

Table S8. Lifetimes and pre-exponential factors obtained from the global analysis from the fluorescence decays for **1-5**.

Molecule/solvent	τ / ns [a]	Pre-exponential factors [b]				
		500 nm	505 nm	530 nm	550 nm	575 nm
1/cyclohexane	0.1-0.3 3.8 ±0.1	0.02 0.98	-	-	0.02 0.98	-
1/CH_3CN[c]	3.9 ± 0.1	1.00	-	1.00	-	-
2/ cyclohexane	0.1-0.3 3.1 ±0.1	0.02 0.98			0.02 0.98	
2/CH_3CN[d]	7.0 ± 0.1	1.00	-	1.00	-	-
3/EtOAc	3.1±0.1 27.0±0.1	-	-	0.02 0.98 (520 nm)	0.01 0.99 (540 nm)	-
3/CH_3CN	23.8 ± 0.1	-	-	1.00 (520 nm)	1.00 (540 nm)	1.00 (580 nm)
4/CH_3CN	11.8 ± 0.1 20.6 ± 0.1	-	-	-	0.17 0.83	0.21 0.79
5/CH_3CN	0.3 ± 0.1 22.6 ± 0.1				0.01 0.99	0.01 0.99

[a] The quoted errors correspond to the maximum absolute deviations. The measurements were performed at 20 °C. [b] Estimated errors on pre-exponential factors range from 5% for the main decay components up to 50% for the minor decay components.

4. Quantum yields of fluorescence and Arrhenius equation

The following equation was used for the determination of fluorescence quantum yields:

$$\Phi = \Phi_R \frac{I}{I_R} \frac{A_R}{A} \left(\frac{n_D}{n_D^R}\right)^2 \quad \text{(S2)}$$

wherein

Φ - quantum yield of fluorescence

Φ_R - quantum yield of fluorescence of reference compound, acridine yellow in methanol

I - intensity of fluorescence (integral of the corrected emission spectrum)

I_R - intensity of fluorescence (integral of the corrected emission spectrum) for the reference compound

A - absorbance of the solution at the excitation wavelength

A_R - absorbance of the solution of the reference compound at the excitation wavelength

n_D - refractive index of the solvent (acetonitrile, cyclohexane or ethyl acetate)

n_D^R - refractive index of the solvent use to dissolve the reference compound (methanol)

Arrhenius equation was used for the estimation of energy barrier for the population of emissive conformers **3B**-**3D**.

$$k = A \exp\left(\frac{E_a}{RT}\right) \quad \text{(S3)}$$

$$\ln k = lnA + \frac{E_a}{RT} \quad \text{(S4)}$$

wherein

k - reaction rate constant

E_a - activation energy

A - pre-exponential factor

R - gas constant (8.314 $JK^{-1}mol^{-1}$)

T - absolute temperature

5. Calculated state energy diagrams for 1-3

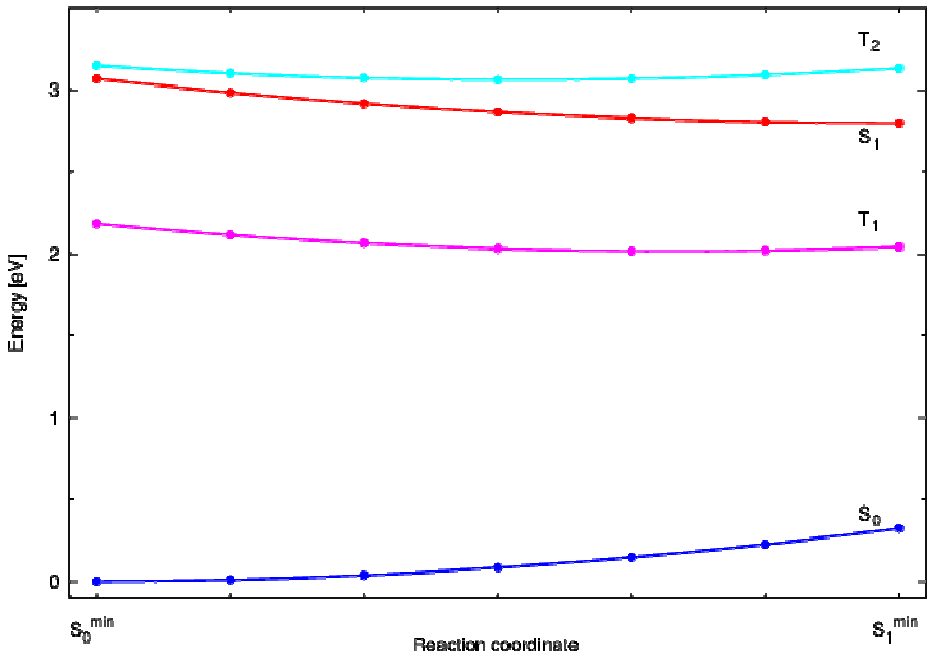

Fig S32. State energy diagram for **1A** including the relevant singlet and triplet states in the region from S_0^{min} to S_1^{min}.

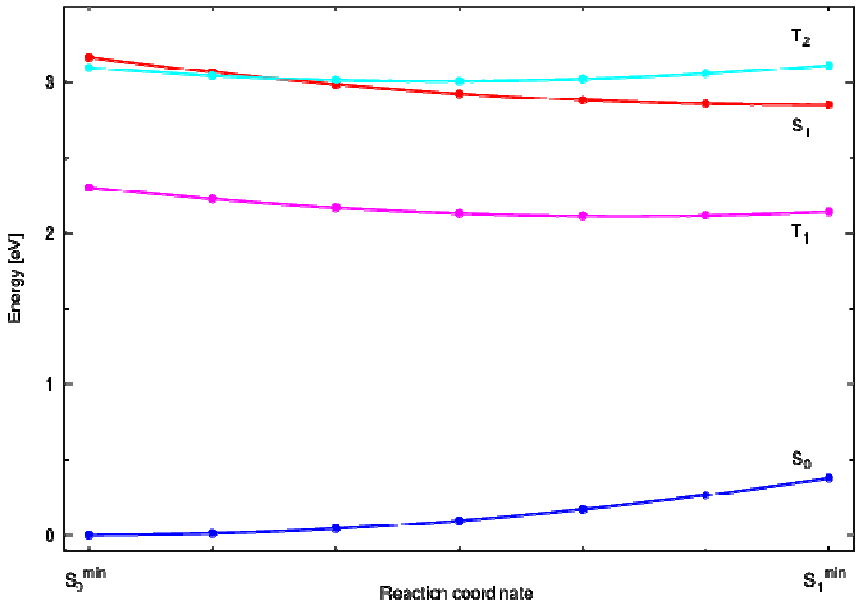

Fig S33. State energy diagram for **2A** including the relevant singlet and triplet states in the region from S_0^{min} to S_1^{min}.

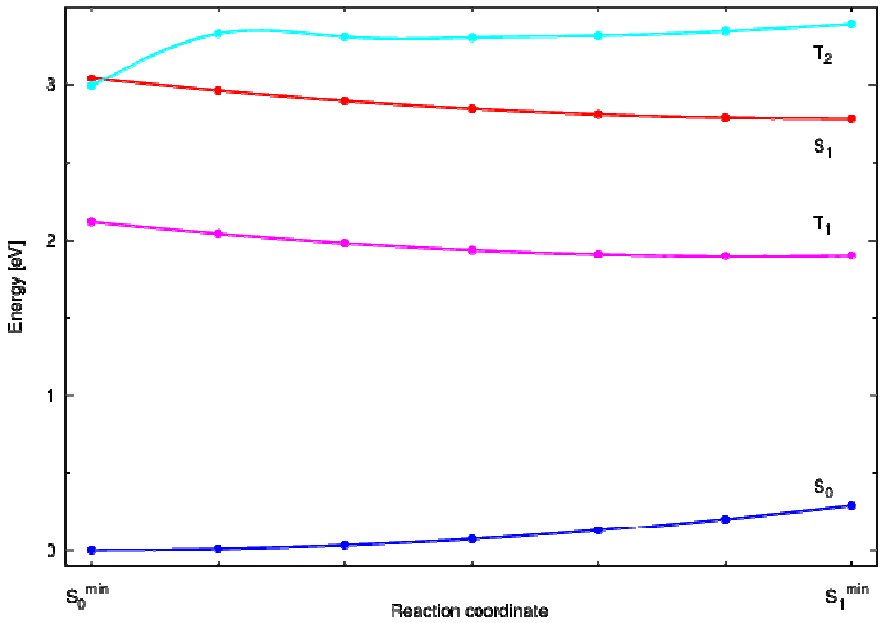

Fig S34. State energy diagram for **3D** including the relevant singlet and triplet states in the region from S_0^{min} to S_1^{min}.

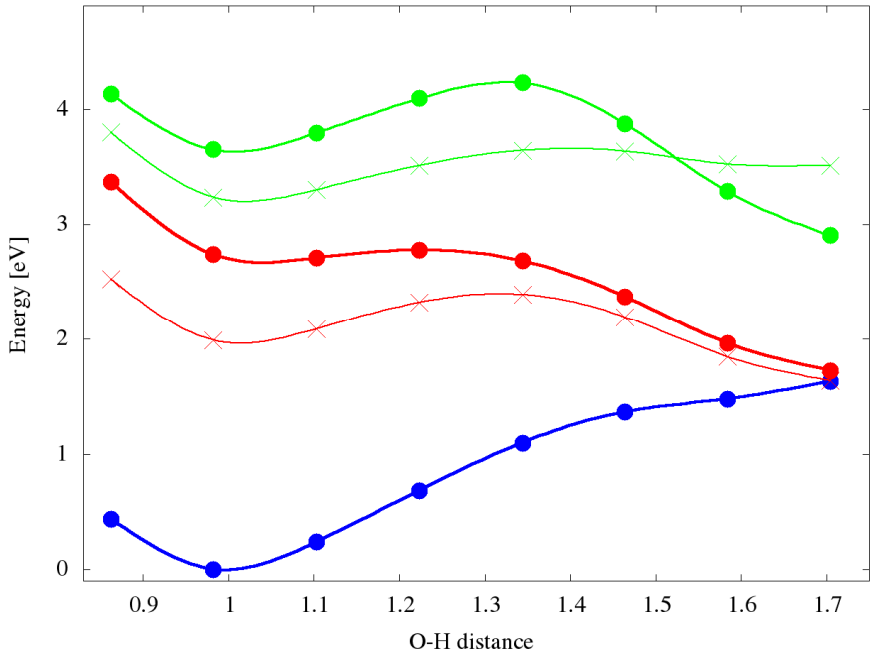

Fig S35. Energy profiles (in eV) of the electronic ground state (S_0, blue), the La(ππ*) (red) and Lb(ππ*) (green) singlet states and the two corresponding triplet states (thin lines) of **3A**. The energy profiles were obtained by linear interpolation in internal coordinates between the FC and CI geometries. The length of the intramolecular hydrogen bond is given in Å.

6. LFP data

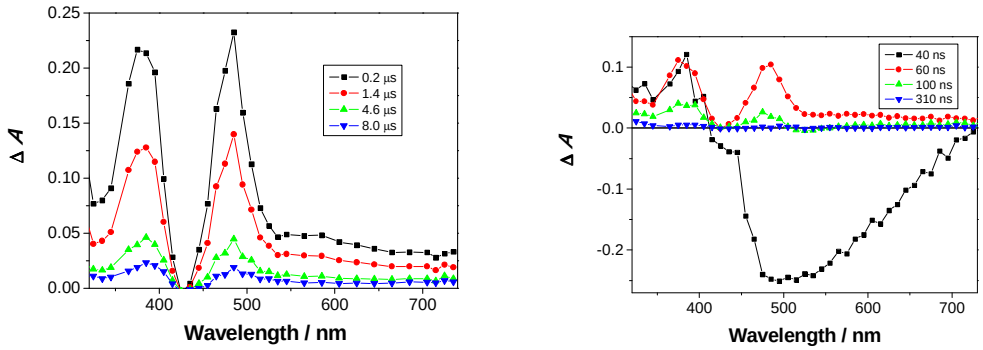

Fig S36. Transient absorption spectra of **1** in optically matched (A_{355} = 0.35) N_2-purged (left) and O_2-purged (right) CH_3CN solution. Due to the detector saturation by fluorescence the intensity of the negative signal at λ>500 nm is not realistic.

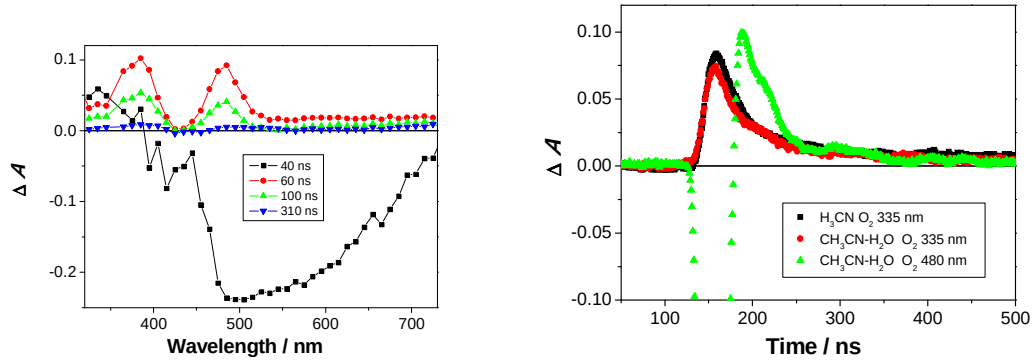

Fig S37. Transient absorption spectra of **1** in O_2-purged CH_3CN-H_2O solution (5:1) (left), and selected decays for N_2-and O_2-purged CH_3CN or CH_3CN-H_2O solution of **1** (right). Due to the detector saturation by fluorescence, the intensity of the negative signal at λ>500 nm is not realistic.

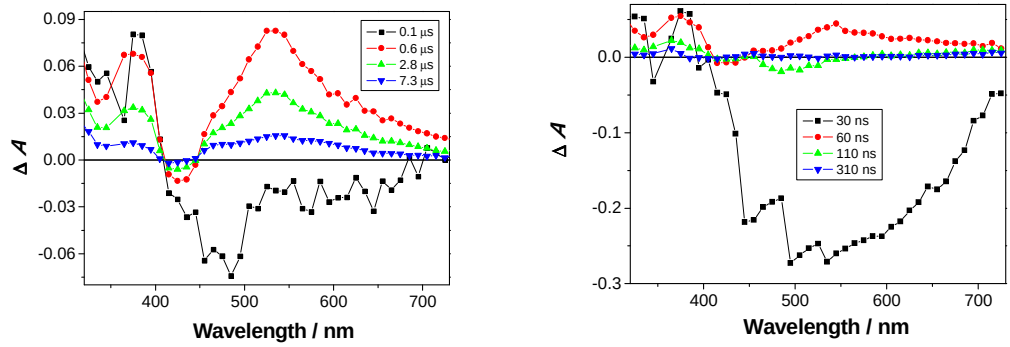

Fig S38. Transient absorption spectra of **2** in optically matched (A_{355} = 0.35) N_2-purged (left) and O_2-purged (right) CH_3CN solution. Due to the detector saturation by fluorescence, the intensity of the negative signal at λ>500 nm is not realistic.

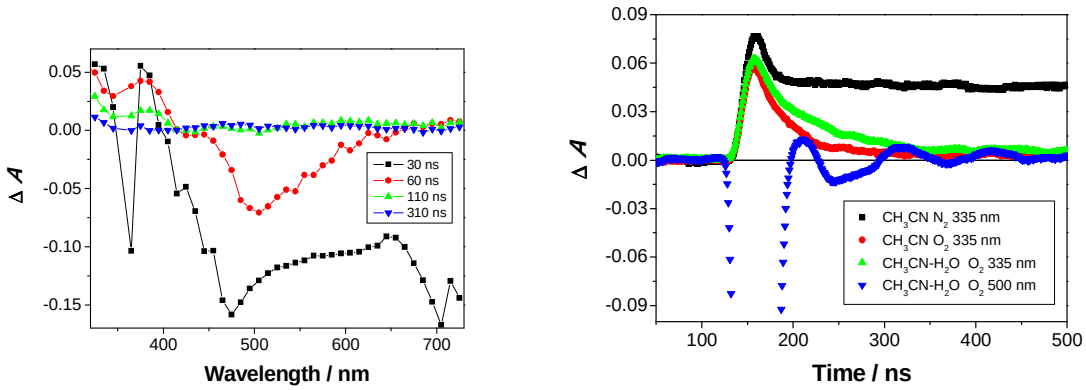

Fig S39. Transient absorption spectra of **2** in O_2-purged CH_3CN-H_2O solution (5:1) (left) and selected decays for N_2-and O_2-purged CH_3CN or CH_3CN-H_2O solution of **2** (right). Due to the detector saturation by fluorescence the intensity of the negative signal at λ>500 nm is not realistic.

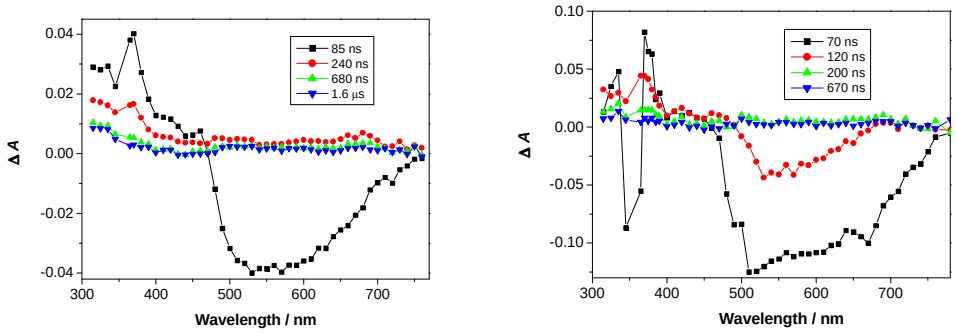

Fig S40. Transient absorption spectra of **3** in N_2-purged (left) and O_2-purged CH_3CN (right), obtained by exciting at 355 nm. Due to the detector saturation by fluorescence, the intensity of the negative signal at λ>500 nm is not realistic.

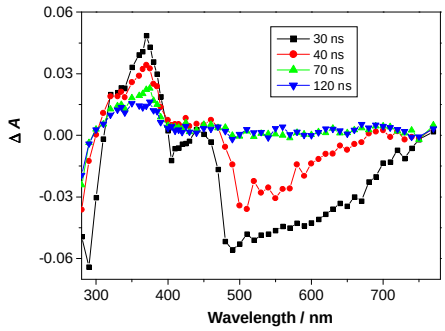

Fig S41. Transient absorption spectra of **3** in O_2-purged CH_3CN obtained by exciting at 266 nm. Due to the detector saturation by fluorescence, the intensity of the negative signal at λ>500 nm is not realistic.

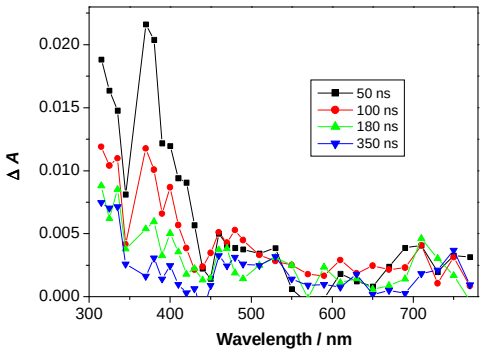

Fig S42. Transient absorption spectra of **3** in O_2-purged CH_3CN-H_2O (1:1) obtained by exciting at 355 nm.

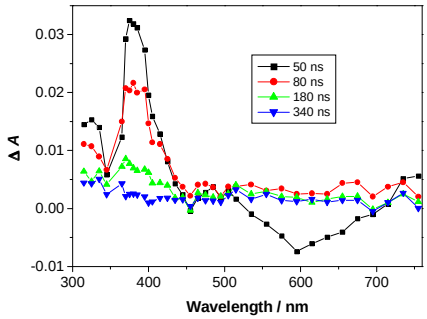

Fig S43. Transient absorption spectra of **3** in O_2-purged CH_3CN-D_2O (1:1), obtained by exciting at 355 nm.

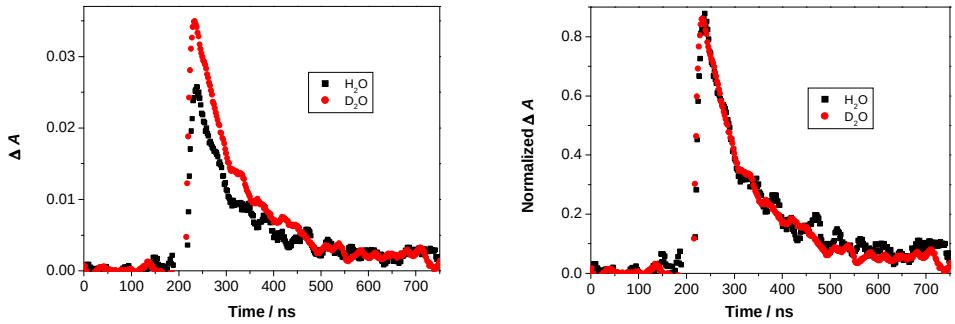

Fig S44. Decays of the transient absorption of **3** at 380 nm for O_2-purged CH_3CN-H_2O and CH_3CN-D_2O solution. The solutions were optically matched at the excitation wavelength (A_{355} = 0.35).

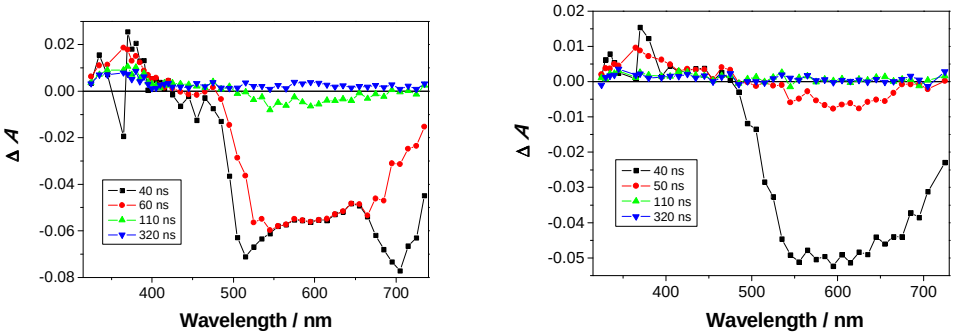

Fig. S45. Transient absorption spectra of **4** in optically matched (A_{355} = 0.35) N_2-purged (left) and O_2-purged (right) CH_3CN solution. Due to the detector saturation by fluorescence, the intensity of the negative signal at λ>500 nm is not realistic.

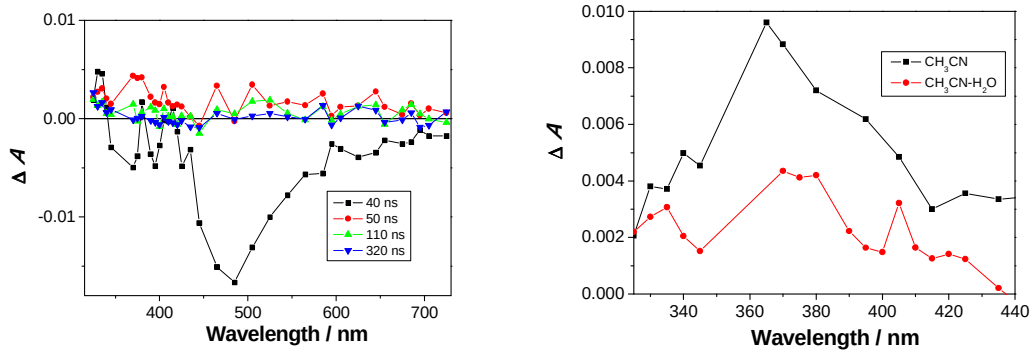

Fig. S46. Transient absorption spectra of **4** in O_2-purged CH_3CN-H_2O (5:1) solution (left), and transient absorption spectra of **4** in optically matched (A_{355} = 0.35) O_2-purged CH_3CN and CH_3CN-H_2O (5:1) solution with the delay of 50 ns (right).

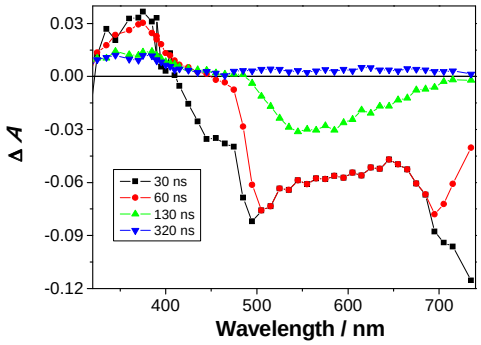

Fig. S47. Transient absorption spectra of **5** in N_2-purged CH_3CN solution. Due to the detector saturation by fluorescence, the intensity of the negative signal at λ>500 nm is not realistic.

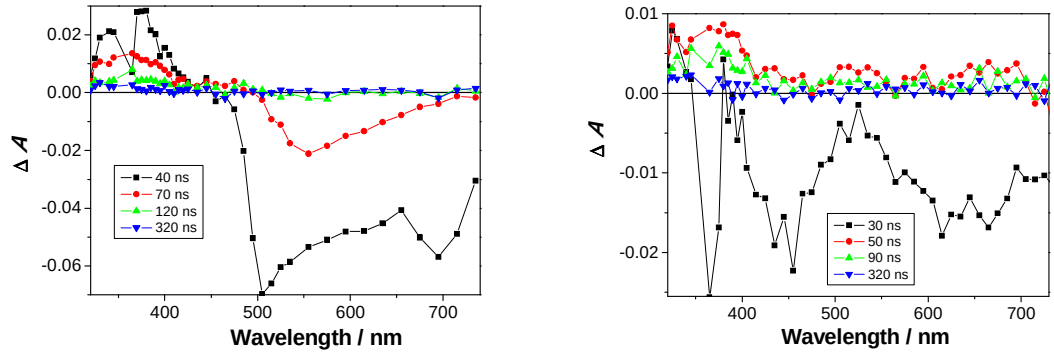

Fig S48. Transient absorption spectra of **5** in optically matched (A_{355} = 0.35) O_2-purged CH_3CN (left) and CH_3CN-H_2O (5:1) solution (right). Due to the detector saturation by fluorescence the intensity of the negative signal is not realistic.

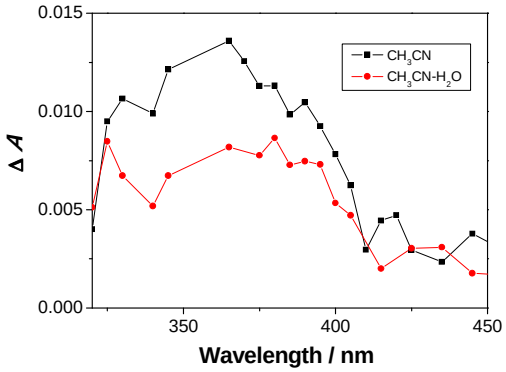

Fig S49. Transient absorption spectra of **5** in optically matched (A_{355} = 0.35) O_2-purged CH_3CN and CH_3CN-H_2O (5:1) solution with the delay of 50 ns (right).

6. Optimized molecular structure coordinates for 1-3

Table S9. Optimized geometry of **1A** in the S_0 state (MP2/aug-cc-pVDZ).

C	-1.8795145	-0.9973731	0.0619418
C	-1.8823852	0.4520809	0.0575076
C	-3.1275225	-1.6946522	0.0572790
C	-0.6476578	-1.6834768	0.0721504
C	0.5804377	-0.9970125	0.0794427
C	0.5643855	0.4497853	0.0735449
C	1.8322873	-1.6993260	0.0937466
C	-3.1371349	1.1392908	0.0489631
C	-0.6555695	1.1496172	0.0626362
C	1.8213968	1.1503843	0.0802902
C	-4.3284137	0.4301530	0.0458683
C	-4.3261642	-0.9987515	0.0500426
C	3.0199338	-1.0013779	0.1022975
C	3.0285398	0.4350743	0.0952933
C	4.2954488	1.1587520	0.1044071
H	-5.2802867	0.9676639	0.0403923
H	-0.6457731	-2.7791316	0.0756599
H	2.7330119	2.7955714	0.0796905
H	5.2178054	0.5394253	0.1174905
H	3.9781218	-1.5296872	0.1143845
H	-5.2743625	-1.5423816	0.0476606
H	-3.1219164	-2.7888860	0.0599855
H	-0.6470130	2.2426887	0.0589962
H	-3.1403165	2.2332167	0.0455471
H	1.8268521	-2.7925128	0.0986121
O	1.7846650	2.4984093	0.0725072
O	4.3941454	2.4014561	0.0986619

Table S10. Optimized geometry of **1B** in the S_0 state, MP2/aug-cc-pVDZ.

C	-1.8794612	-0.9996134	0.0632101
C	-1.8782866	0.4493444	0.0588586
C	-3.1285919	-1.6937958	0.0577469
C	-0.6485165	-1.6873336	0.0733896
C	0.5787976	-1.0009249	0.0805293
C	0.5698489	0.4453970	0.0754003
C	1.8312917	-1.6987019	0.0935839

C	-3.1310436	1.1394520	0.0487311
C	-0.6508794	1.1457989	0.0648523
C	1.8275318	1.1420816	0.0814896
C	-4.3245869	0.4339025	0.0442444
C	-4.3257370	-0.9947853	0.0492203
C	3.0177783	-1.0010137	0.1007717
C	3.0341451	0.4366256	0.0937531
C	4.3414386	1.1208894	0.0987714
H	-5.2750036	0.9740854	0.0372517
H	-0.6463016	-2.7828657	0.0767661
H	2.5989536	2.9100226	0.0811359
H	4.3318923	2.2391325	0.0849200
H	3.9821134	-1.5136237	0.1114234
H	-5.2753130	-1.5360291	0.0460178
H	-3.1258699	-2.7880623	0.0613606
H	-0.6487308	2.2383302	0.0621450
H	-3.1318094	2.2334278	0.0451631
H	1.8285239	-2.7920554	0.0979342
O	1.7175642	2.5110925	0.0745236
O	5.4292527	0.5452226	0.1158055

Table S11. Optimized geometry of **1C** in the S_0 state, MP2/aug-cc-pVDZ.

C	-1.8913689	-1.0037272	0.0612978
C	-1.9082725	0.4444001	0.0551686
C	-3.1323867	-1.7134177	0.0577326
C	-0.6505758	-1.6701173	0.0723490
C	0.5712196	-0.9702165	0.0793237
C	0.5556030	0.4810167	0.0724333
C	1.8206065	-1.6648724	0.0943292
C	-3.1688415	1.1203882	0.0467087
C	-0.6859518	1.1512809	0.0592761
C	1.8144275	1.1860827	0.0799406
C	-4.3537311	0.4003424	0.0455278
C	-4.3370032	-1.0283390	0.0509993
C	3.0022472	-0.9537728	0.1013019
C	3.0218305	0.4787007	0.0930805
C	4.3586464	1.1275705	0.1001439
H	-5.3103339	0.9290576	0.0413329
H	-0.6320976	-2.7655939	0.0768152

H	0.9540434	2.8882311	0.0733072
H	5.1974106	0.3888719	0.1180304
H	3.9616052	-1.4798027	0.1133561
H	-5.2798335	-1.5809944	0.0498566
H	-3.1159642	-2.8074058	0.0615624
H	-0.7511101	2.2456083	0.0520033
H	-3.1858238	2.2144817	0.0424443
H	1.8223964	-2.7578855	0.1011114
O	1.8603198	2.5476969	0.0754168
O	4.5979397	2.3314157	0.0881498

Table S12. Optimized geometry of **1D** in the S_0 state, MP2/aug-cc-pVDZ.

C	-1.8913035	-1.0025729	0.0621463
C	-1.9004115	0.4453630	0.0559784
C	-3.1357242	-1.7050600	0.0581082
C	-0.6542073	-1.6778424	0.0732385
C	0.5712156	-0.9864519	0.0797912
C	0.5613292	0.4645887	0.0722153
C	1.8196979	-1.6883566	0.0942991
C	-3.1568321	1.1281093	0.0474404
C	-0.6735985	1.1448811	0.0597868
C	1.8264152	1.1505361	0.0784695
C	-4.3459576	0.4146629	0.0456135
C	-4.3370809	-1.0136515	0.0507478
C	3.0097986	-0.9932605	0.1004979
C	3.0261653	0.4387270	0.0917919
C	4.3298357	1.1479183	0.0974106
H	-5.2995742	0.9487025	0.0407992
H	-0.6434959	-2.7733446	0.0778569
H	0.9940233	2.8803664	0.0703257
H	4.2862197	2.2556695	0.0882008
H	3.9737526	-1.5069803	0.1121743
H	-5.2827571	-1.5614453	0.0488741
H	-3.1251181	-2.7990660	0.0616507
H	-0.7297893	2.2398275	0.0525700
H	-3.1679611	2.2223154	0.0432916
H	1.8103415	-2.7816609	0.1011094
O	1.8924136	2.5227150	0.0715186
O	5.4136045	0.5613102	0.1110930

Table S13. Optimized geometry of **2A** in the S_0 state, MP2/aug-cc-pVDZ.

C	-1.718625	-1.268332	-0.014320
C	-1.733260	0.178314	-0.020327
C	-2.960825	-1.976025	-0.016872
C	-0.475804	-1.930691	-0.003423
C	0.734806	-1.212973	0.005258
C	0.731761	0.235768	-0.001050
C	1.988297	-1.911367	0.022338
C	-2.992299	0.856124	-0.027192
C	-0.514609	0.892182	-0.016175
C	2.005831	0.932973	0.009868
C	-4.181834	0.142877	-0.025674
C	-4.162957	-1.285664	-0.020828
C	3.186835	-1.234418	0.032133
C	3.203238	0.195435	0.024690
C	2.094418	2.389794	0.011414
H	-5.137480	0.673148	-0.027758
H	-0.445902	-3.025830	0.000901
H	4.254815	1.757206	0.028612
H	1.150450	2.965699	0.008309
H	4.145648	-1.757433	0.046574
H	-5.106424	-1.837793	-0.019796
H	-2.947096	-3.070026	-0.013923
H	-0.578423	1.982711	-0.023314
H	-3.003939	1.950614	-0.031730
H	1.976774	-3.005477	0.028804
O	4.419335	0.775811	0.034481
O	3.170271	3.024372	0.017999

Table S14. Optimized geometry of **2B** in the S_0 state, MP2/aug-cc-pVDZ.

C	-1.709410	-1.271504	-0.010034
C	-1.711335	0.175125	-0.015147
C	-2.956945	-1.970170	-0.014806
C	-0.471253	-1.938927	-0.000066
C	0.743612	-1.226599	0.007335
C	0.759688	0.225794	0.003745
C	1.986123	-1.932920	0.019344
C	-2.965796	0.862911	-0.025129

C	-0.490696	0.883543	-0.008931
C	2.031416	0.928059	0.013876
C	-4.160419	0.158987	-0.029276
C	-4.153021	-1.270259	-0.023874
C	3.182475	-1.249886	0.029115
C	3.214075	0.178411	0.026794
C	2.067024	2.413814	0.011553
H	-5.111938	0.696594	-0.036122
H	-0.444828	-3.034086	0.003039
H	5.116806	0.142947	0.044163
H	1.074362	2.909632	0.002232
H	4.129843	-1.799662	0.039240
H	-5.100841	-1.814795	-0.026819
H	-2.952006	-3.064268	-0.010195
H	-0.559274	1.972277	-0.013679
H	-2.968968	1.957356	-0.028707
H	1.975929	-3.026695	0.021379
O	4.421877	0.818400	0.037888
O	3.080499	3.110920	0.019084

Table S15. Optimized geometry of **2C** in the S_0 state, MP2/aug-cc-pVDZ

C	-1.7282578	-1.2772292	-0.0088133
C	-1.7457658	0.1708251	-0.0140592
C	-2.9689928	-1.9909663	-0.0141772
C	-0.4805516	-1.9345804	0.0018389
C	0.7278912	-1.2088890	0.0085368
C	0.7198460	0.2435740	0.0041851
C	1.9806381	-1.9047314	0.0204654
C	-3.0084170	0.8452558	-0.0253655
C	-0.5310113	0.8980977	-0.0078835
C	1.9895915	0.9577762	0.0142116
C	-4.1967548	0.1262172	-0.0306747
C	-4.1747715	-1.3034189	-0.0248262
C	3.1744598	-1.2167291	0.0289630
C	3.1819545	0.2114009	0.0255112
C	2.0815319	2.4301730	0.0167669
H	-5.1551232	0.6537739	-0.0392103
H	-0.4433691	-3.0305736	0.0054892
H	4.4271404	1.6970691	0.0239542

H	3.1199847	2.8467991	0.0446047
H	4.1384547	-1.7320040	0.0376732
H	-5.1177263	-1.8586098	-0.0287157
H	-2.9525983	-3.0860844	-0.0095647
H	-0.5694668	1.9879671	-0.0127350
H	-3.0206184	1.9403650	-0.0294682
H	1.9776865	-2.9998404	0.0226480
O	4.4549474	0.7298328	0.0329961
O	1.1522989	3.2415306	-0.0053509

Table S16. Optimized geometry of **2D** in the S_0 state, MP2/aug-cc-pVDZ.

C	-1.720259	-1.277401	-0.014331
C	-1.730947	0.169944	-0.019006
C	-2.962836	-1.984448	-0.017084
C	-0.479113	-1.942240	-0.003951
C	0.732159	-1.223933	0.005160
C	0.731250	0.228489	0.000876
C	1.979406	-1.922625	0.021295
C	-2.990254	0.848702	-0.026400
C	-0.514921	0.890125	-0.013230
C	1.996630	0.934870	0.013067
C	-4.180636	0.135704	-0.025951
C	-4.164543	-1.293146	-0.021229
C	3.174806	-1.234919	0.031280
C	3.182985	0.191025	0.026117
C	2.126746	2.412986	0.017869
H	-5.135918	0.666859	-0.028846
H	-0.450050	-3.037509	-0.000872
H	5.100306	0.204012	0.045242
H	3.172697	2.778475	0.035266
H	4.126280	-1.776776	0.044265
H	-5.108754	-1.844399	-0.020421
H	-2.950179	-3.078608	-0.014268
H	-0.541015	1.979755	-0.017675
H	-2.996949	1.942903	-0.030785
H	1.975175	-3.016675	0.026731
O	4.388084	0.858884	0.034650
O	1.196850	3.224949	0.006231

Table S17. Optimized geometry of **3A** in the S_0 state, MP2/aug-cc-pVDZ.

C	-1.9511218	-0.7061116	-0.0210988
C	-1.9473314	0.7452629	-0.0302939
C	-3.2058330	-1.3955725	-0.0251138
C	-0.7242615	-1.3981189	-0.0079284
C	0.5019176	-0.7012480	-0.0026584
C	0.5137222	0.7509201	-0.0117036
C	1.7518792	-1.3822586	0.0133814
C	-3.1998451	1.4383410	-0.0431342
C	-0.7184462	1.4363238	-0.0258455
C	1.7595363	1.4474612	-0.0050750
C	-4.3969719	0.7403190	-0.0471508
C	-4.3976418	-0.6895090	-0.0379222
C	2.9549860	-0.6817686	0.0207966
C	2.9622802	0.7597630	0.0108116
C	4.2090488	-1.4507711	0.0414720
H	1.7770130	2.5407518	-0.0111738
H	-0.7209035	-2.4936925	-0.0006863
H	4.0925724	-2.5568971	0.0478307
H	4.8602727	0.7967391	0.0303445
H	-5.3485754	-1.2288752	-0.0410886
H	-5.3456060	1.2829827	-0.0572537
H	-3.2076437	-2.4896769	-0.0174742
H	-0.7214864	2.5318857	-0.0326238
H	-3.1965858	2.5326296	-0.0495543
H	1.7702346	-2.4783411	0.0215732
O	4.1331612	1.4569328	0.0172429
O	5.3406298	-0.9464708	0.0523263

Table S18. Optimized geometry of **3B** in the S_0 state, MP2/aug-cc-pVDZ.

C	-1.7523285	-0.8164601	0.0025913
C	-1.8201322	0.6318978	-0.0676102
C	-2.9714347	-1.5628233	0.0801880
C	-0.4945906	-1.4505864	-0.0073956
C	0.6964174	-0.6982398	-0.0851320
C	0.6333388	0.7497245	-0.1554994
C	1.9756177	-1.3204144	-0.0969711
C	-3.1035775	1.2650759	-0.0564594

C	-0.6274426	1.3789507	-0.1448800
C	1.8452721	1.4964848	-0.2337092
C	-4.2644916	0.5125811	0.0195199
C	-4.1952560	-0.9140161	0.0882998
C	3.1486201	-0.5749357	-0.1738924
C	3.0741371	0.8609494	-0.2434627
C	4.4444544	-1.3054810	-0.1799779
H	1.8170312	2.5882849	-0.2875818
H	-0.4374743	-2.5432370	0.0456979
H	5.3757560	-0.6915677	-0.2357648
H	4.9928653	1.1383836	-0.3225463
H	-5.1183244	-1.4966869	0.1478706
H	-5.2381437	1.0091407	0.0271169
H	-2.9201982	-2.6543991	0.1331119
H	-0.6827425	2.4718226	-0.1978095
H	-3.1537736	2.3569918	-0.1093116
H	2.0601807	-2.4103712	-0.0450348
O	4.1886122	1.6729403	-0.3227027
O	4.5536067	-2.5280087	-0.1276541

Table S19. Optimized geometry of **3C** in the S_0 state, MP2/aug-cc-pVDZ

C	-1.9413988	-0.7043601	0.3487057
C	-1.9424088	0.7454577	0.2979747
C	-3.1924396	-1.3968267	0.3797487
C	-0.7119784	-1.3927858	0.3675780
C	0.5095909	-0.6923959	0.3384856
C	0.5137606	0.7547868	0.2845929
C	1.7653366	-1.3661300	0.3611206
C	-3.1949394	1.4354080	0.2834429
C	-0.7157926	1.4399422	0.2656941
C	1.7649963	1.4427489	0.2540504
C	-4.3896984	0.7342462	0.3169165
C	-4.3863956	-0.6941813	0.3652165
C	2.9751619	-0.6821476	0.3325948
C	2.9685584	0.7573113	0.2769194
C	4.2073703	-1.5190252	0.3627594
H	1.7660935	2.5379230	0.2123238
H	-0.7044510	-2.4876210	0.4062278
H	3.9786756	-2.6122316	0.4104890

H	4.0295759	2.3416248	0.2142861
H	-5.3357362	-1.2357060	0.3904747
H	-5.3401813	1.2737300	0.3067696
H	-3.1911076	-2.4903083	0.4157816
H	-0.7226997	2.5348690	0.2265445
H	-3.1954409	2.5290715	0.2451295
H	1.7810262	-2.4613600	0.4032082
O	4.1860518	1.3856101	0.2499538
O	5.3674712	-1.1256498	0.3400088

Table S20. Optimized geometry of **3D** in the S_0 state, MP2/aug-cc-pVDZ

C	-1.7842263	-0.7300660	-0.1671953
C	-1.7820152	0.7197033	-0.1112840
C	-3.0371210	-1.4180592	-0.2245064
C	-0.5579062	-1.4234225	-0.1629659
C	0.6681174	-0.7303533	-0.1053700
C	0.6739930	0.7187118	-0.0504013
C	1.9168068	-1.4178087	-0.0992362
C	-3.0325220	1.4138960	-0.1142100
C	-0.5532743	1.4084876	-0.0549444
C	1.9255230	1.4060073	0.0071129
C	-4.2287815	0.7169066	-0.1691665
C	-4.2286589	-0.7115260	-0.2250549
C	3.1211704	-0.7316603	-0.0427541
C	3.1166009	0.7040320	0.0110430
C	4.4053761	-1.4952752	-0.0390209
H	1.9312095	2.5010065	0.0484705
H	-0.5536603	-2.5179838	-0.2045622
H	5.3336800	-0.8917749	0.0077653
H	4.2250853	2.2703326	0.0987678
H	-5.1792585	-1.2495851	-0.2685063
H	-5.1777899	1.2591111	-0.1698486
H	-3.0384036	-2.5112495	-0.2673794
H	-0.5563490	2.5034146	-0.0134039
H	-3.0300950	2.5074422	-0.0713585
H	1.9458635	-2.5111772	-0.1395276
O	4.3552084	1.3113792	0.0653004
O	4.4574269	-2.7234889	-0.0847628

Table S21. Optimized geometry of **1A** in the S_1 state, ADC(2)/aug-cc-pVDZ

C	-1.9147351	-1.0038145	0.0629375
C	-1.9134170	0.4421885	0.0578923
C	-3.1373788	-1.6932314	0.0579979
C	-0.6471484	-1.6861504	0.0737946
C	0.5693576	-0.9931617	0.0803686
C	0.5721901	0.4693120	0.0745740
C	1.8188783	-1.6745375	0.0932983
C	-3.1478973	1.1229616	0.0486738
C	-0.6655774	1.1500631	0.0630033
C	1.8074229	1.1546568	0.0811172
C	-4.3689191	0.4099601	0.0444192
C	-4.3675782	-0.9919255	0.0488671
C	3.0430678	-0.9684962	0.1010629
C	3.0916414	0.4282809	0.0955704
C	4.3265842	1.1541904	0.1037550
H	-5.3136587	0.9599377	0.0377405
H	-0.6352583	-2.7820583	0.0777843
H	2.8323349	2.7333358	0.0826419
H	5.2634329	0.5605857	0.1152947
H	3.9845081	-1.5290021	0.1118799
H	-5.3096467	-1.5461016	0.0455305
H	-3.1342552	-2.7880206	0.0616324
H	-0.6706646	2.2453472	0.0586248
H	-3.1540544	2.2176971	0.0451565
H	1.8283539	-2.7684831	0.0978790
O	1.8388369	2.4905874	0.0749499
O	4.3865813	2.4248788	0.0985531

Table S22. Optimized geometry of **1B** in the S_1 state, ADC(2)/aug-cc-pVDZ

C	-1.9159363	-1.0112072	0.0637955
C	-1.9069747	0.4375627	0.0588793
C	-3.1422795	-1.6952249	0.0581845
C	-0.6524889	-1.6911210	0.0748692
C	0.5707908	-0.9977228	0.0811132
C	0.5828308	0.4646120	0.0753177
C	1.8173816	-1.6725379	0.0935007

C	-3.1403796	1.1211955	0.0489663
C	-0.6620777	1.1422816	0.0642931
C	1.8160079	1.1475876	0.0812200
C	-4.3660367	0.4127703	0.0437445
C	-4.3716672	-0.9887392	0.0481762
C	3.0330615	-0.9546305	0.0996167
C	3.0927427	0.4509681	0.0934748
C	4.3847030	1.1154784	0.0992616
H	-5.3077630	0.9678353	0.0362814
H	-0.6376662	-2.7869813	0.0791177
H	2.6602709	2.8643664	0.0814039
H	4.3739178	2.2371794	0.0917952
H	3.9869733	-1.4918177	0.1093187
H	-5.3158693	-1.5389382	0.0441344
H	-3.1428410	-2.7899391	0.0618161
H	-0.6762788	2.2371724	0.0601568
H	-3.1438118	2.2160438	0.0454344
H	1.8367909	-2.7663326	0.0984795
O	1.7571346	2.5090481	0.0752707
O	5.4884657	0.5370909	0.1113774

Table S23. Optimized geometry of **1C** in the S_1 state, ADC(2)/aug-cc-pVDZ

C	-1.9221200	-1.0152872	0.0622256
C	-1.9364025	0.4331723	0.0560504
C	-3.1438836	-1.7076138	0.0585640
C	-0.6500696	-1.6821656	0.0730092
C	0.5639141	-0.9778071	0.0795537
C	0.5621536	0.4825786	0.0728146
C	1.8179029	-1.6404914	0.0939000
C	-3.1741262	1.1068594	0.0471386
C	-0.6924817	1.1449122	0.0599291
C	1.8018381	1.1749500	0.0806090
C	-4.3948524	0.3888355	0.0445621
C	-4.3795375	-1.0108999	0.0501190
C	3.0341025	-0.9181366	0.1012874
C	3.0840830	0.4781654	0.0941091
C	4.3980196	1.1295379	0.1002208
H	-5.3427188	0.9330339	0.0384701
H	-0.6253817	-2.7776852	0.0779800

H	0.9722912	2.8833453	0.0703893
H	5.2365187	0.3895827	0.1146680
H	3.9803862	-1.4694518	0.1127087
H	-5.3169607	-1.5734447	0.0481883
H	-3.1365856	-2.8023800	0.0628804
H	-0.7641407	2.2413972	0.0529226
H	-3.1872836	2.2021401	0.0427203
H	1.8407501	-2.7342466	0.0996168
O	1.8738245	2.5175744	0.0774429
O	4.6357614	2.3425249	0.0909196

Table S24. Optimized geometry of **1D** in the S_1 state, ADC(2)/aug-cc-pVDZ

C	-1.9240164	-1.0155129	0.0631970
C	-1.9263490	0.4342509	0.0568742
C	-3.1489071	-1.7026976	0.0591065
C	-0.6564044	-1.6884946	0.0742545
C	0.5622700	-0.9897010	0.0800527
C	0.5714222	0.4716720	0.0730366
C	1.8110568	-1.6620405	0.0933160
C	-3.1629421	1.1124534	0.0475312
C	-0.6819355	1.1403740	0.0607827
C	1.8168995	1.1444930	0.0792963
C	-4.3862331	0.3992592	0.0443485
C	-4.3820333	-1.0012544	0.0499115
C	3.0343634	-0.9519174	0.0993498
C	3.0855933	0.4473489	0.0922010
C	4.3772945	1.1444640	0.0980074
H	-5.3308037	0.9495120	0.0376652
H	-0.6363249	-2.7842648	0.0793457
H	1.0138915	2.8785158	0.0664419
H	4.3350814	2.2533139	0.0903497
H	3.9864687	-1.4912706	0.1098569
H	-5.3230537	-1.5572112	0.0473973
H	-3.1451948	-2.7975758	0.0635628
H	-0.7486392	2.2371756	0.0543101
H	-3.1724120	2.2077764	0.0430843
H	1.8241051	-2.7561860	0.0991455
O	1.9074158	2.4975344	0.0740594
O	5.4703884	0.5559834	0.1105148

Table S25. Optimized geometry of **2A** in the S_1 state, ADC(2)/aug-cc-pVDZ

C	-1.7355975	-1.2509830	-0.0129720
C	-1.7624781	0.1880693	-0.0189107
C	-2.9479191	-1.9592045	-0.0156772
C	-0.4609866	-1.9133058	-0.0021673
C	0.7605620	-1.2262960	0.0065822
C	0.7379976	0.2410353	0.0004168
C	1.9975531	-1.9295722	0.0221513
C	-2.9979627	0.8580616	-0.0266721
C	-0.5148019	0.8936321	-0.0147768
C	1.9905019	0.9415211	0.0111939
C	-4.2130508	0.1313757	-0.0271821
C	-4.1849641	-1.2688473	-0.0219374
C	3.2418769	-1.2460635	0.0318910
C	3.2552381	0.1402137	0.0255904
C	2.0926681	2.3690009	0.0114991
H	-5.1665274	0.6652940	-0.0311879
H	-0.4460911	-3.0101491	0.0017828
H	4.1627440	1.7972842	0.0284074
H	1.1590766	2.9607987	0.0048117
H	4.1925239	-1.7833300	0.0440506
H	-5.1180816	-1.8380459	-0.0221432
H	-2.9335046	-3.0537540	-0.0117989
H	-0.5656228	1.9853178	-0.0222063
H	-3.0155171	1.9525526	-0.0311027
H	1.9732217	-3.0243124	0.0269244
O	4.4089467	0.8070775	0.0329549
O	3.1931957	3.0096305	0.0194781

Table S26. Optimized geometry of **2B** in the S_1 state, ADC(2)/aug-cc-pVDZ

C	-1.7332592	-1.2727514	-0.0095297
C	-1.7481930	0.1699258	-0.0142216
C	-2.9745241	-1.9750004	-0.0153229
C	-0.4849627	-1.9402051	0.0011418
C	0.7310270	-1.2340147	0.0084067
C	0.7141156	0.2172180	0.0043679
C	1.9814222	-1.9349830	0.0200660
C	-2.9970730	0.8521383	-0.0249014

C	-0.5139299	0.8747003	-0.0073662
C	2.0067288	0.9371108	0.0136268
C	-4.1951953	0.1437416	-0.0301243
C	-4.1788316	-1.2794738	-0.0251437
C	3.2019636	-1.2407126	0.0287250
C	3.2259233	0.1511289	0.0259272
C	2.0901431	2.2942579	0.0117436
H	-5.1481775	0.6788770	-0.0379246
H	-0.4626835	-3.0358490	0.0043575
H	5.1449970	0.2975162	0.0437816
H	1.2337973	2.9802504	0.0031169
H	4.1464545	-1.7962486	0.0379500
H	-5.1227447	-1.8314566	-0.0290093
H	-2.9664753	-3.0691861	-0.0114947
H	-0.5639021	1.9684130	-0.0111919
H	-3.0042643	1.9469204	-0.0286115
H	1.9754956	-3.0288665	0.0225146
O	4.3834056	0.8997790	0.0345382
O	3.2857433	3.0617717	0.0205778

Table S27. Optimized geometry of **2C** in the S_1 state, ADC(2)/aug-cc-pVDZ

C	-1.7217690	-1.2634002	-0.0079040
C	-1.7317228	0.1787775	-0.0169013
C	-2.9639484	-1.9599266	-0.0118928
C	-0.4756183	-1.9434987	0.0050019
C	0.7441752	-1.2494046	0.0104749
C	0.7309955	0.2035753	0.0032988
C	1.9974638	-1.9448502	0.0215173
C	-2.9742353	0.8663476	-0.0297444
C	-0.4878027	0.8753076	-0.0122485
C	2.0097092	0.9255384	0.0156778
C	-4.1763910	0.1605780	-0.0326616
C	-4.1679761	-1.2604757	-0.0238595
C	3.2162420	-1.2440141	0.0252108
C	3.2418327	0.1458137	0.0218552
C	2.1063422	2.2785252	0.0259974
H	-5.1265882	0.7008139	-0.0420100
H	-0.4660665	-3.0394233	0.0111245
H	5.1528843	0.2731281	0.0366055

H	3.0488457	2.8393381	0.0382535
H	4.1619140	-1.7981917	0.0312540
H	-5.1140046	-1.8087393	-0.0267143
H	-2.9603519	-3.0543757	-0.0055393
H	-0.5161989	1.9744435	-0.0220200
H	-2.9751749	1.9610125	-0.0366105
H	1.9977579	-3.0390300	0.0262859
O	4.4018130	0.8850920	0.0264664
O	1.0048738	3.1720404	0.0230824

Table S28. Optimized geometry of **2D** in the S_1 state, ADC(2)/aug-cc-pVDZ

C	-1.7384264	-1.2563661	-0.0093231
C	-1.7606742	0.1827431	-0.0144671
C	-2.9498132	-1.9680359	-0.0149804
C	-0.4677356	-1.9132732	0.0021785
C	0.7575373	-1.2234331	0.0096132
C	0.7397413	0.2386999	0.0050110
C	1.9893292	-1.9334401	0.0220175
C	-2.9977057	0.8506186	-0.0255625
C	-0.5197981	0.8962222	-0.0078658
C	1.9817913	0.9606648	0.0150410
C	-4.2122722	0.1202467	-0.0310510
C	-4.1883062	-1.2800841	-0.0256581
C	3.2218363	-1.2288694	0.0294198
C	3.2217416	0.1551840	0.0256601
C	2.0563178	2.4017329	0.0168962
H	-5.1656559	0.6546420	-0.0393263
H	-0.4479625	-3.0103698	0.0059749
H	4.3207052	1.7243870	0.0245211
H	3.0877548	2.8404588	0.0330065
H	4.1807334	-1.7518209	0.0369672
H	-5.1218241	-1.8483144	-0.0295854
H	-2.9331150	-3.0627939	-0.0108261
H	-0.5258484	1.9887364	-0.0120283
H	-3.0138856	1.9448083	-0.0296484
H	1.9747272	-3.0279248	0.0251419
O	4.4397510	0.7619848	0.0317212
O	1.1040575	3.2205974	0.0041525

Table S29. Geometry of **3A** S_1/S_0 CI, ADC(2)/aug-cc-pVDZ

C	-1.9945037	-0.6779502	-0.0272708
C	-2.0132390	0.7510314	-0.0335979
C	-3.2113428	-1.3821414	-0.0293023
C	-0.7130153	-1.3675209	-0.0157746
C	0.4792387	-0.6731729	-0.0088336
C	0.4601273	0.7801106	-0.0185030
C	1.7618491	-1.3637609	0.0104566
C	-3.2416426	1.4316746	-0.0397040
C	-0.7436191	1.4561016	-0.0311514
C	1.7278280	1.4763221	-0.0125956
C	-4.4572355	0.7175782	-0.0396419
C	-4.4365654	-0.6846736	-0.0349765
C	2.9853600	-0.6848432	0.0228229
C	2.9672994	0.7996953	0.0084838
C	4.2132335	-1.3812411	0.0488644
H	1.7549336	2.5706846	-0.0227655
H	-0.7105638	-2.4640568	-0.0100383
H	4.2483847	-2.4758550	0.0608318
H	5.2128551	0.1975002	0.0481381
H	-5.3748121	-1.2459864	-0.0350130
H	-5.4074113	1.2573378	-0.0428021
H	-3.2027702	-2.4764135	-0.0251938
H	-0.7515378	2.5521326	-0.0379968
H	-3.2504188	2.5263378	-0.0435192
H	1.7502407	-2.4620119	0.0188315
O	4.0740242	1.4652773	0.0159353
O	5.4183038	-0.7811555	0.0623157

Table S30. Optimized geometry of **3B** in the S_1 state, ADC(2)/aug-cc-pVDZ

C	-1.7749328	-0.7958604	0.0004404
C	-1.8564010	0.6441140	-0.0655418
C	-2.9632300	-1.5425171	0.0763469
C	-0.4829946	-1.4313152	-0.0126186
C	0.7177208	-0.7073109	-0.0875413
C	0.6261601	0.7546817	-0.1561170
C	1.9866352	-1.3357676	-0.0988557
C	-3.1153726	1.2665775	-0.0519872

C	-0.6304783	1.3875239	-0.1437586
C	1.8325179	1.4863446	-0.2339731
C	-4.3026988	0.4990378	0.0252849
C	-4.2242457	-0.8980103	0.0886324
C	3.2153478	-0.6031483	-0.1750038
C	3.0859993	0.8207861	-0.2422807
C	4.4848240	-1.2898755	-0.1812013
H	1.8345614	2.5785359	-0.2892483
H	-0.4406467	-2.5262710	0.0382729
H	5.4069756	-0.6523709	-0.2427373
H	4.9636704	1.1160797	-0.3187269
H	-5.1350075	-1.4994553	0.1479820
H	-5.2741341	0.9995081	0.0345645
H	-2.9090091	-2.6347676	0.1265181
H	-0.6764409	2.4813320	-0.1954798
H	-3.1735776	2.3585833	-0.1016230
H	2.0559308	-2.4280753	-0.0478372
O	4.1482575	1.6474359	-0.3191162
O	4.6265682	-2.5297945	-0.1233935

Table S31. Optimized geometry of **3C** in the S_1 state, ADC(2)/aug-cc-pVDZ

C	-1.9741151	-0.7099974	0.3492993
C	-1.9584820	0.7346904	0.3008253
C	-3.2306410	-1.3842593	0.3796773
C	-0.7470026	-1.4150447	0.3662717
C	0.4891863	-0.7358639	0.3382782
C	0.5013561	0.7203704	0.2885431
C	1.7208339	-1.4336659	0.3587252
C	-3.1926073	1.4407411	0.2849929
C	-0.7084671	1.4125530	0.2708462
C	1.7702153	1.4146602	0.2588298
C	-4.4049920	0.7578897	0.3161012
C	-4.4200487	-0.6643813	0.3636870
C	2.9762420	-0.7296885	0.3308930
C	2.9519844	0.7247771	0.2791598
C	4.1619350	-1.4178599	0.3544810
H	1.7723971	2.5096767	0.2203185
H	-0.7563268	-2.5105194	0.4027580
H	4.2263729	-2.5147258	0.3952037

H	4.1127266	2.2588994	0.2231084
H	-5.3756339	-1.1954217	0.3883980
H	-5.3463766	1.3132496	0.3040441
H	-3.2450833	-2.4779085	0.4165165
H	-0.7025748	2.5081015	0.2337029
H	-3.1772620	2.5347595	0.2483079
H	1.7285349	-2.5289028	0.3973516
O	4.2052452	1.2930253	0.2547662
O	5.4715843	-0.8531546	0.3319109

Table S32. Optimized geometry of **3D** in the S_1 state, ADC(2)/aug-cc-pVDZ

C	-1.8011139	-0.7099891	-0.1656344
C	-1.8129674	0.7346910	-0.1089817
C	-3.0250151	-1.3977495	-0.2218126
C	-0.5437736	-1.4062471	-0.1626883
C	0.6966462	-0.7416924	-0.1045477
C	0.6748812	0.7236362	-0.0469668
C	1.9296772	-1.4285512	-0.1005838
C	-3.0403353	1.4158027	-0.1135779
C	-0.5526995	1.4169550	-0.0502572
C	1.9180475	1.3901920	0.0102974
C	-4.2663606	0.7054979	-0.1711317
C	-4.2558576	-0.6928605	-0.2244612
C	3.1942038	-0.7551197	-0.0435132
C	3.1428388	0.6618600	0.0115155
C	4.4404979	-1.5039344	-0.0452980
H	1.9522579	2.4853465	0.0542244
H	-0.5546353	-2.5023537	-0.2082565
H	5.3743514	-0.9042447	0.0037428
H	4.1324980	2.2890652	0.0979199
H	-5.1947816	-1.2507031	-0.2678531
H	-5.2122505	1.2529596	-0.1732974
H	-3.0244243	-2.4917573	-0.2641058
H	-0.5461607	2.5122345	-0.0058934
H	-3.0453197	2.5097129	-0.0721905
H	1.9469642	-2.5231662	-0.1423891
O	4.3145456	1.3361571	0.0665829
O	4.4942850	-2.7487413	-0.0978416

7. NMR spectra

^{1}H NMR ($CDCl_3$, 300 MHz) spectra of 4-oxo-4-(5,6,7,8-tetrahydronaphthalen-2-yl)butanoic acid (**6**).

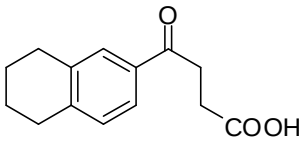

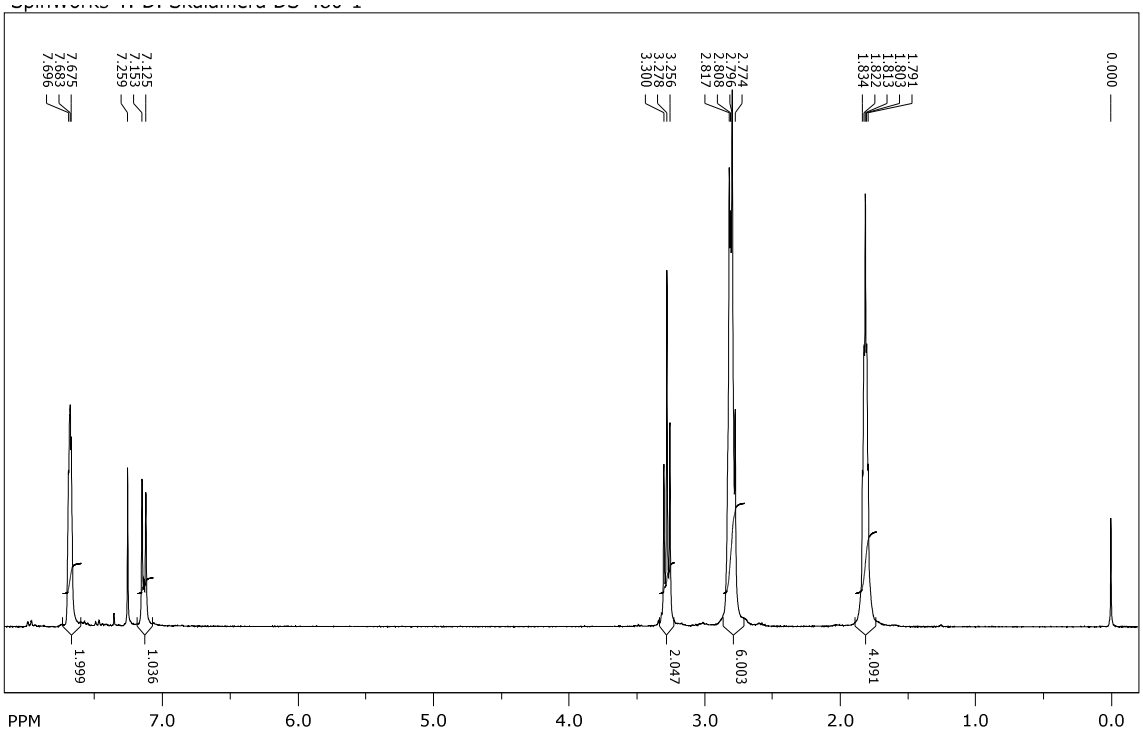

^{1}H NMR ($CDCl_3$, 600 MHz) of 4-(5,6,7,8-tetrahydronaphthalen-2-yl)butanoic acid (**7**).

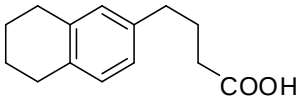

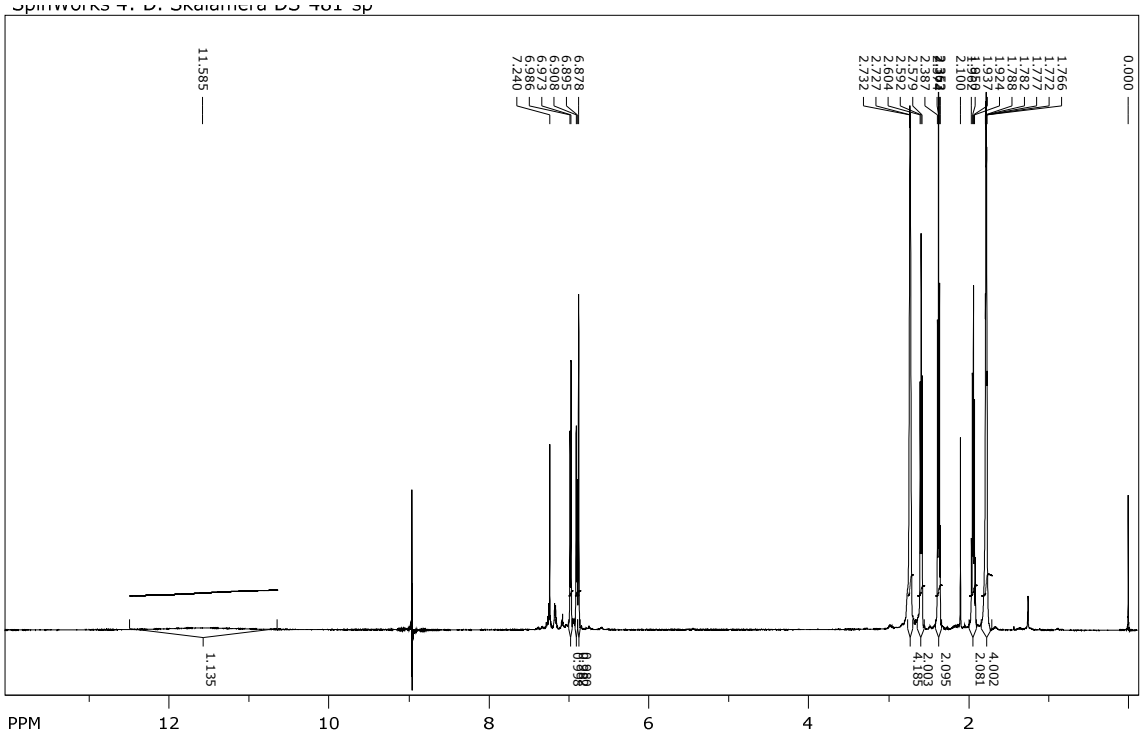

^{1}H NMR ($CDCl_3$, 300 MHz) spectra of 3,4,5,6,7,8-hexahydroanthracen-1(2*H*)-one (**8**).

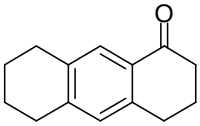

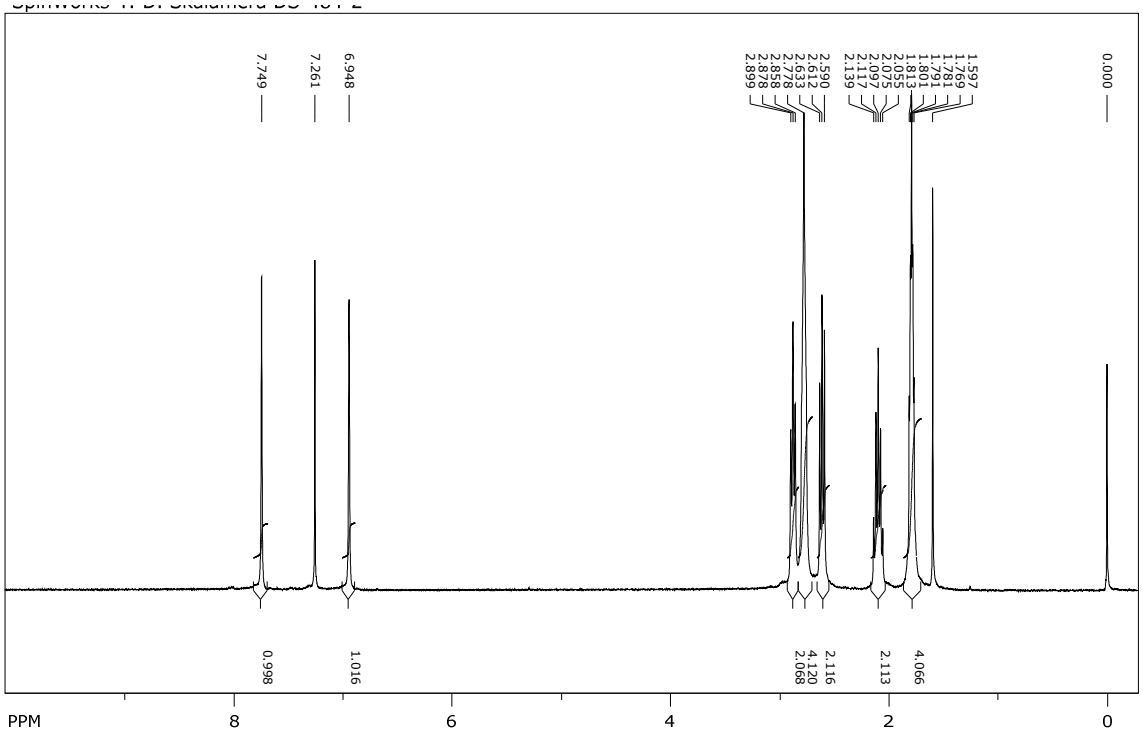

^{1}H NMR ($CDCl_3$, 300 MHz) spectra of
2-(hydroxymethylene)-3,4,5,6,7,8-hexahydroanthracen-1(*2H*)-one (**9**).

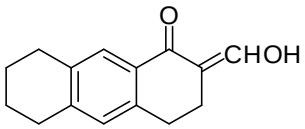

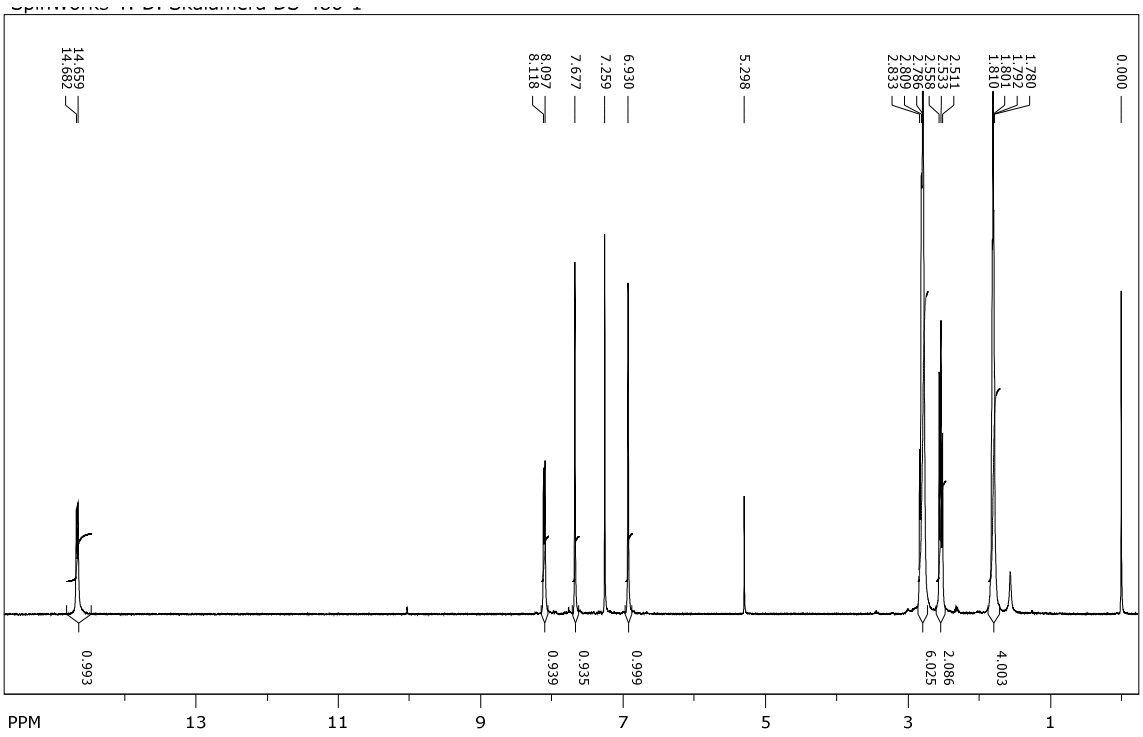

^{1}H NMR ($CDCl_3$, 600 MHz) spectra of 1-hydroxyanthracene-2-carbaldehyde (**1**).

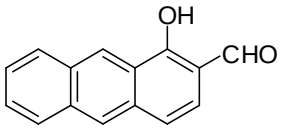

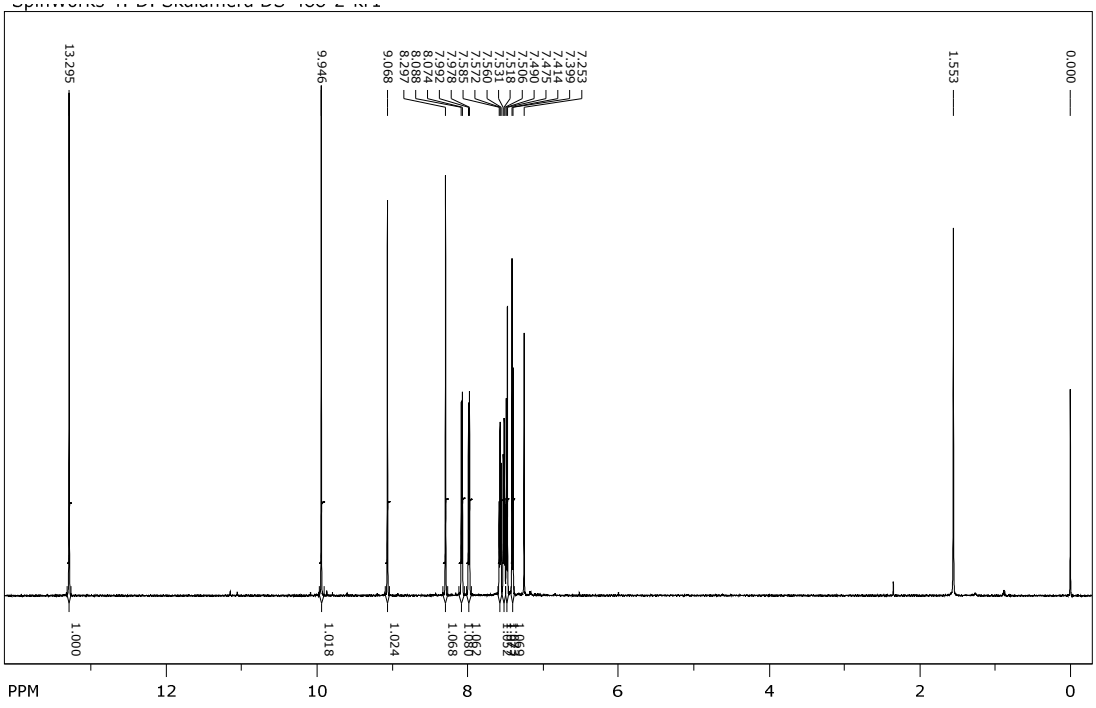

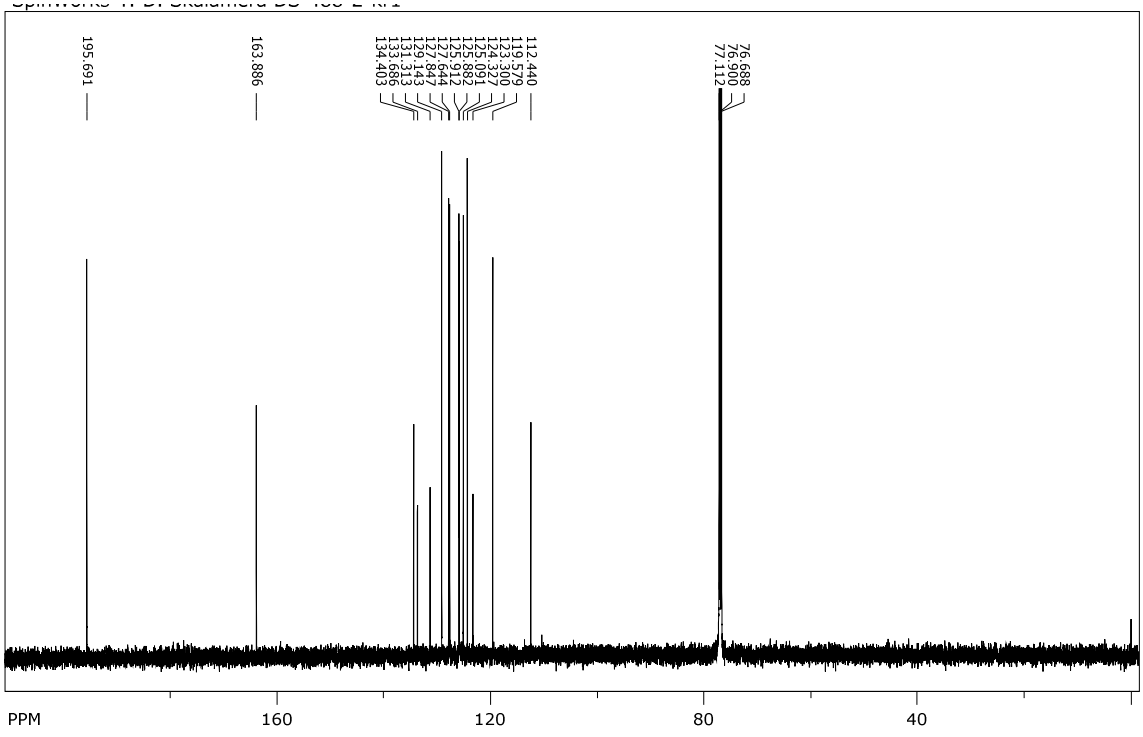

^{1}H NMR ($CDCl_3$, 600 MHz) spectra of 2-anthrol (**10**).

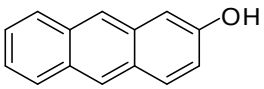

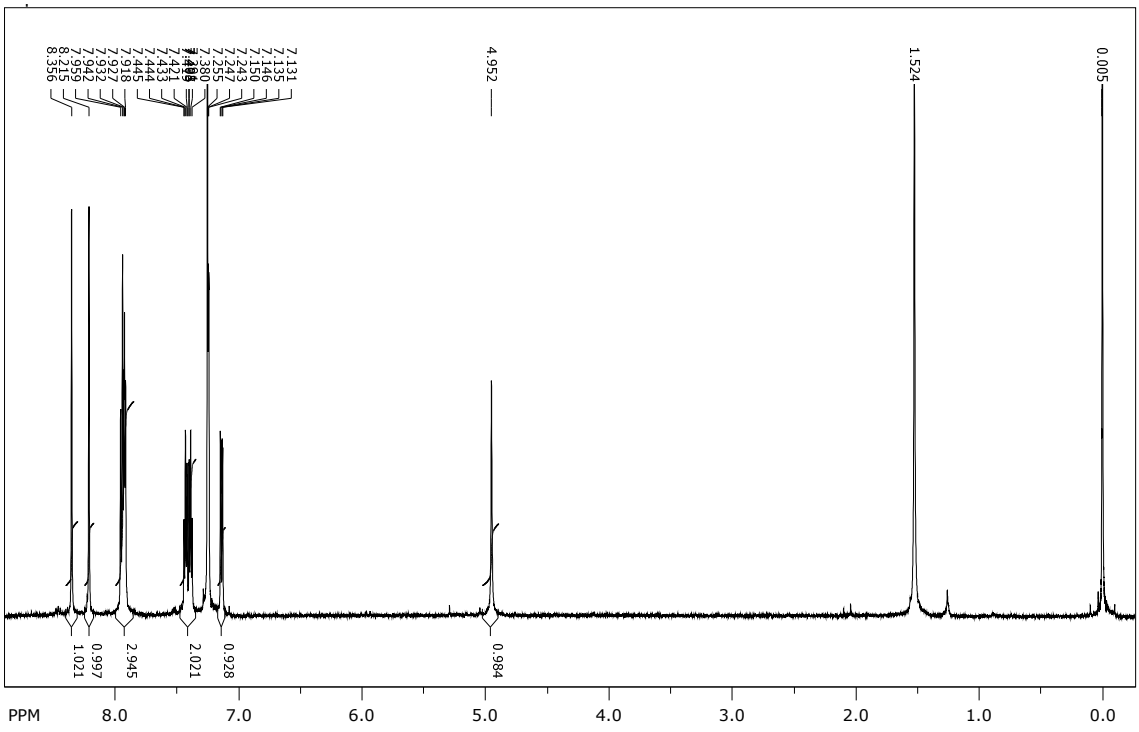

^{1}H NMR ($CDCl_3$, 600 MHz) and ^{13}C NMR ($CDCl_3$, 600 MHz) spectra of 2-Hydroxyanthracene-1-carbaldehyde (**2**).

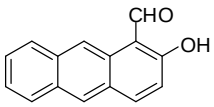

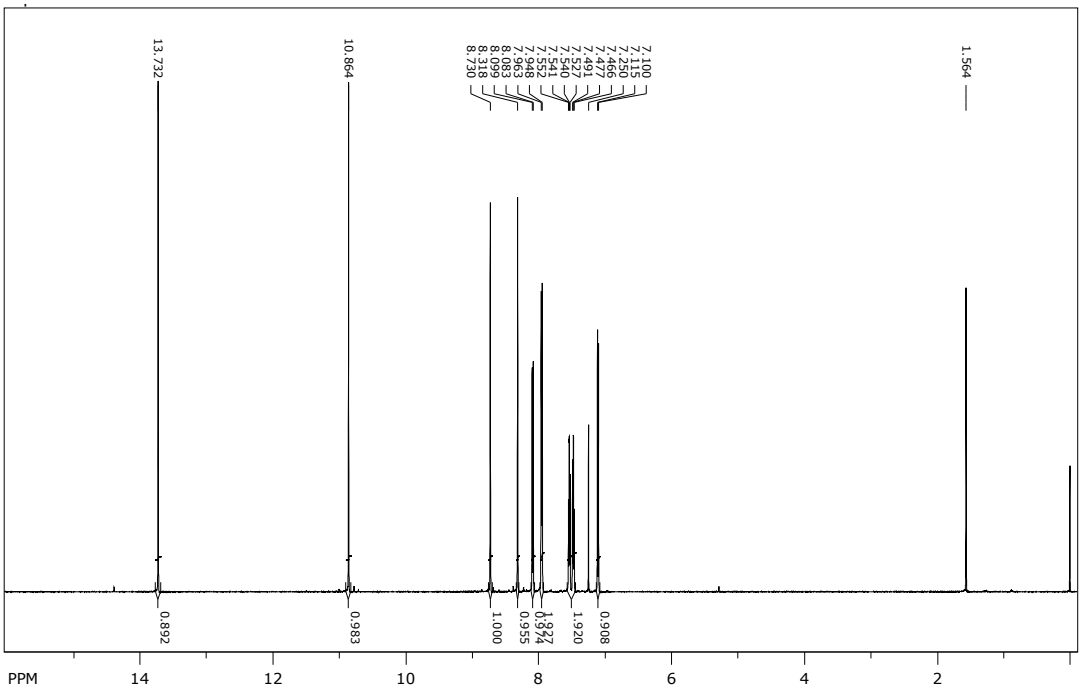

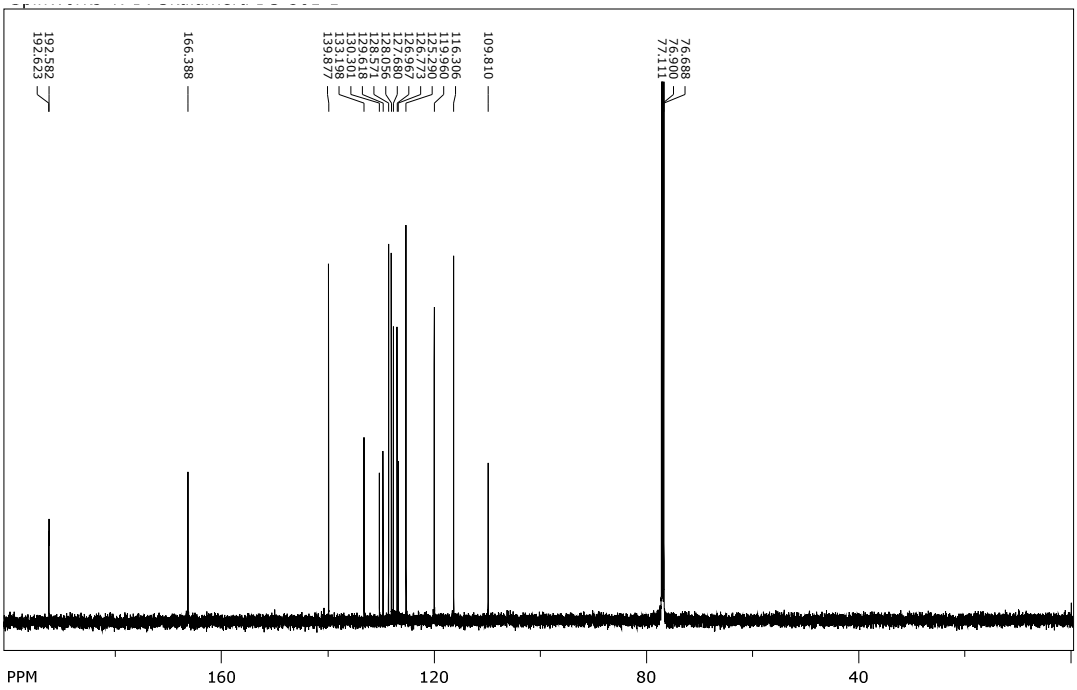

^{1}H NMR (300 MHz, $CDCl_3$) and ^{13}C NMR (75 MHz, $CDCl_3$) spectra of 3-hydroxyanthracene-2-carbaldehyde (**3**)

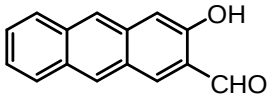

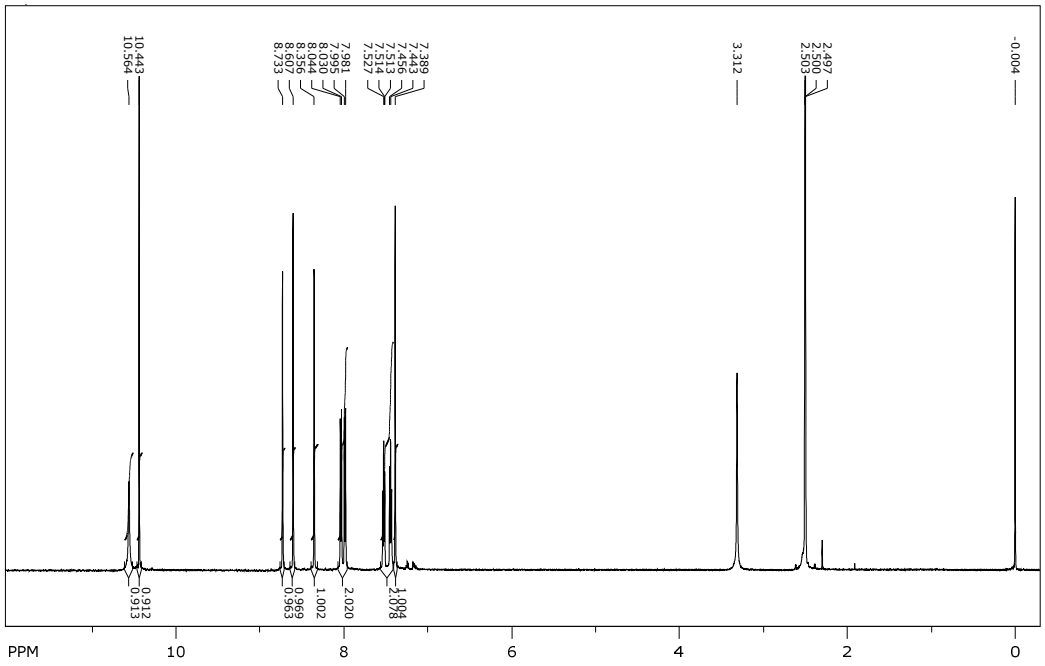

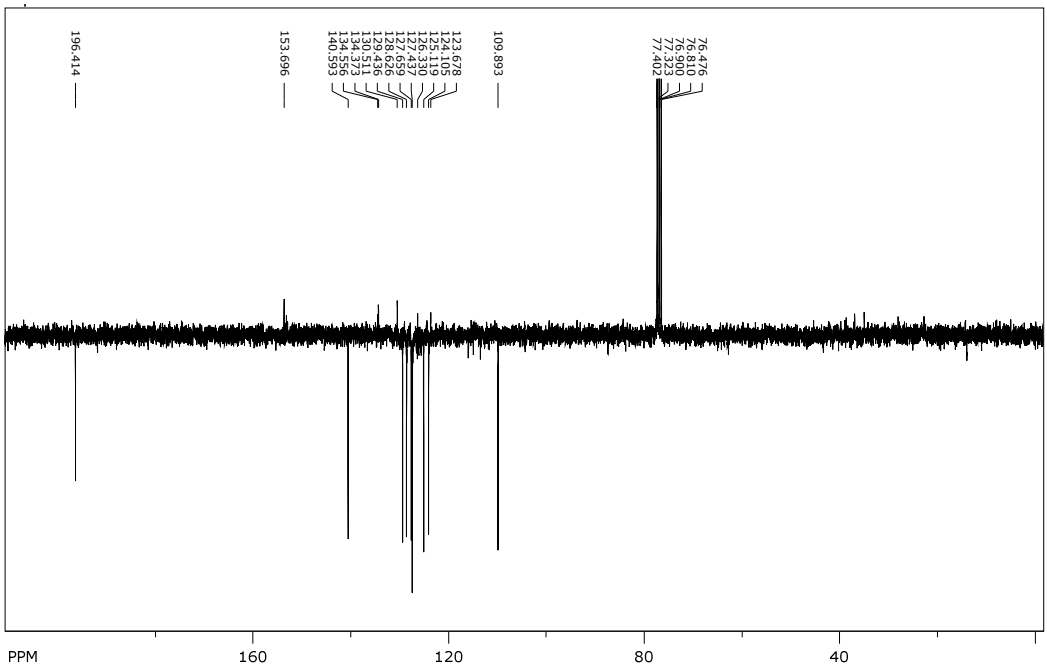

^{1}H NMR (300 MHz, $CDCl_3$) and ^{13}C NMR (75 MHz, $CDCl_3$) spectra of 9,10-dimethyl-2-hydroxyanthracene-3-carbaldehyde (**4**).

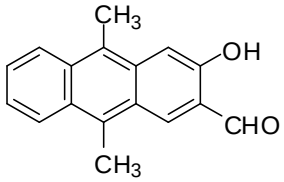

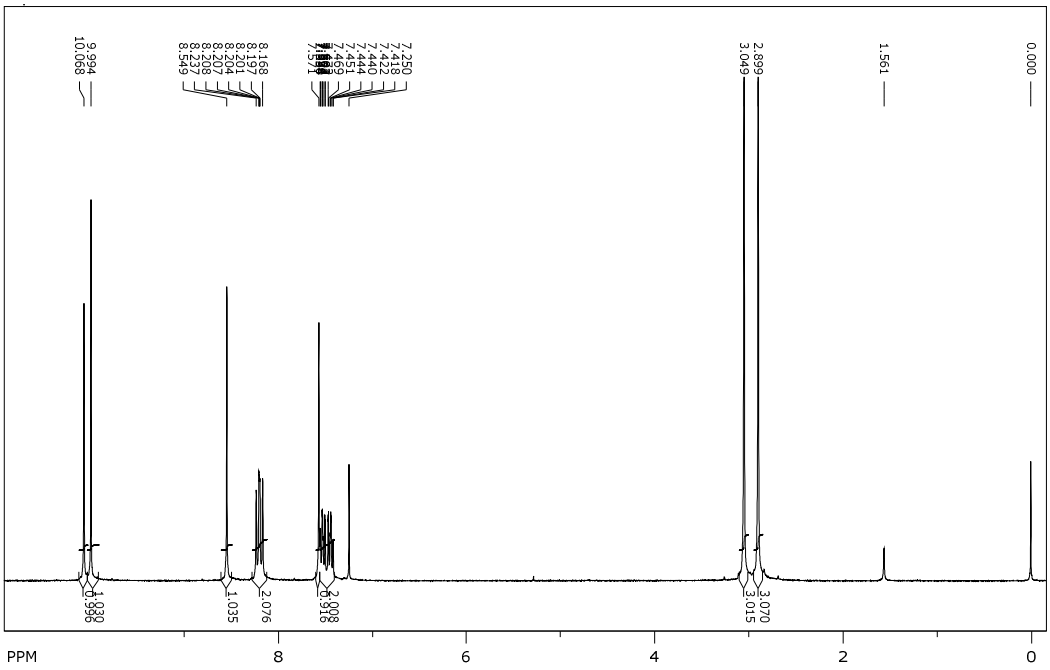

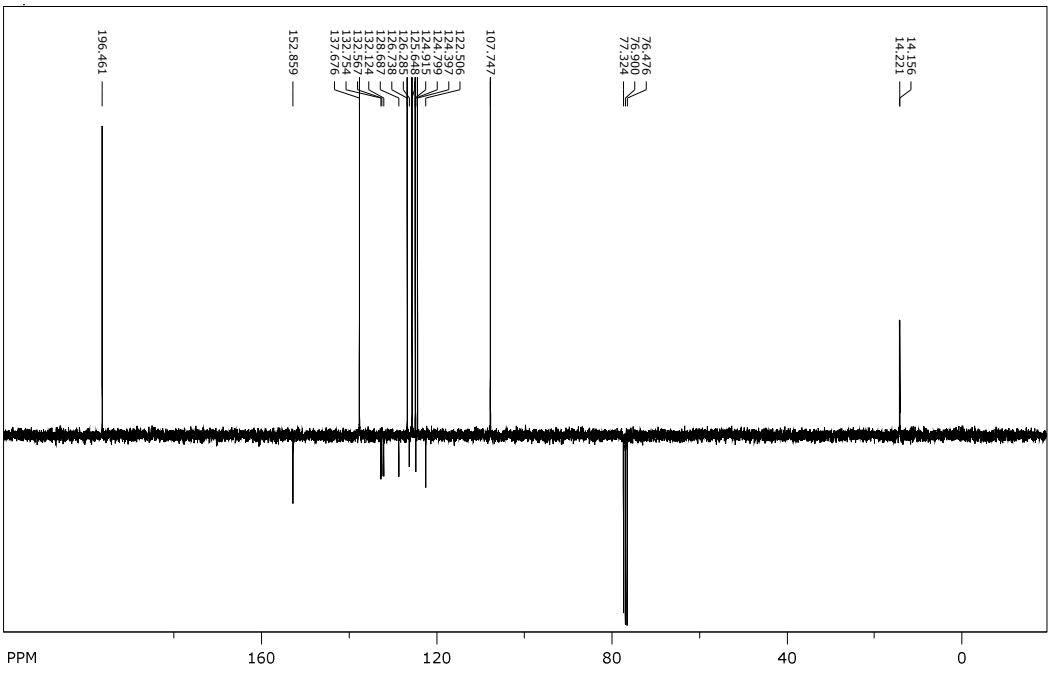

^{1}H NMR (600 MHz, $CDCl_3$) and ^{13}C NMR (150 MHz, $CDCl_3$) spectra of 9,10-diphenyl-2-hydroxyanthracene-3-carbaldehyde (**5**).

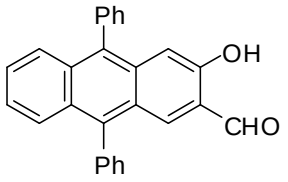

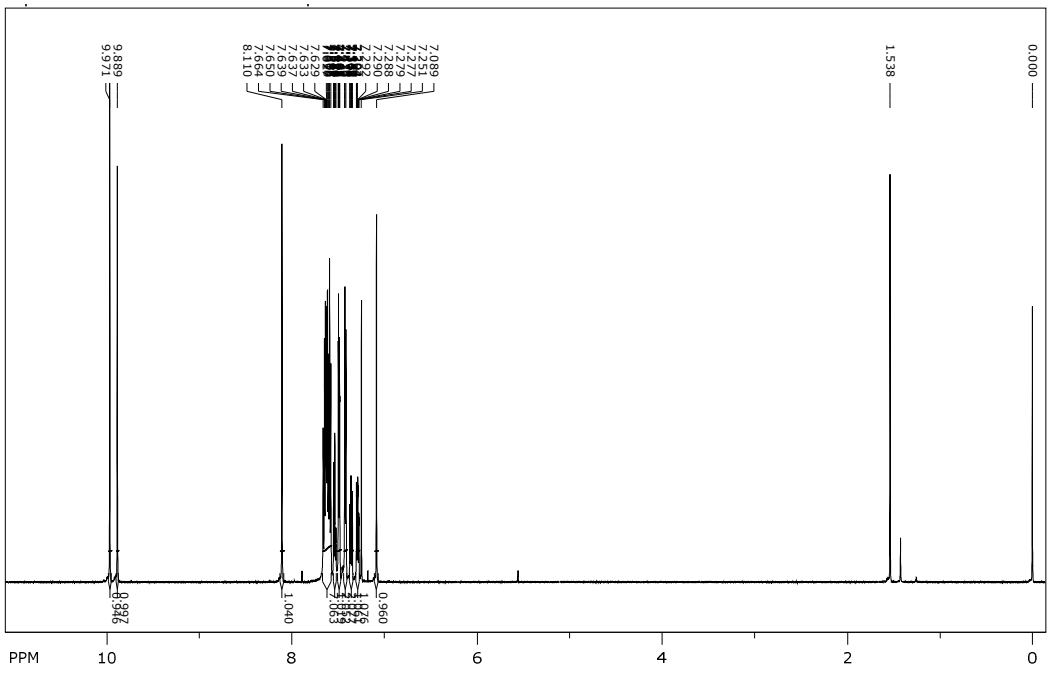

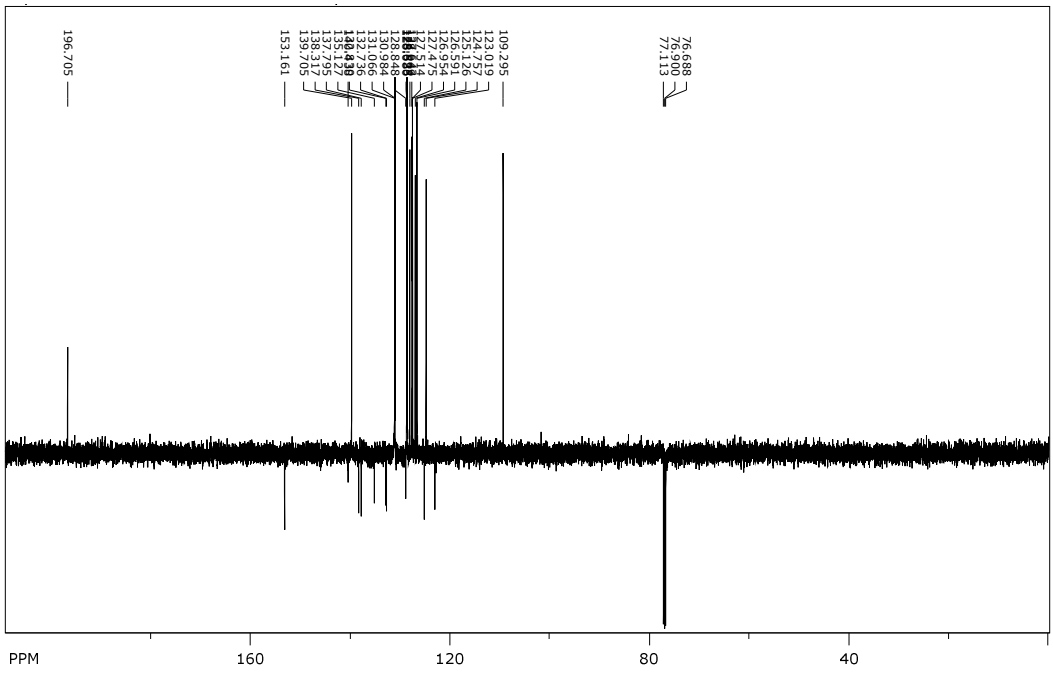

9. References

[1] C. Biliger, P. Demerseman, R. Royer, *J. Heterocycl. Chem.,* 1985, **22**, 735-739.

[2] M. S. Newman, H. V. Zahm, *J. Am. Chem. Soc.*, 1943, **65**, 1097-1101.

[3] E. L. Martin, *J. Am. Chem. Soc.*, 1936, **58**, 1438-1442.

[4] Z. Zhang, R. Sangaiah, A. Gold, L. M. Ball, *Org. Biomol. Chem.,* 2011, **9**, 5431-5435.

[5] A. W. Burgstahler, E. Mosettig, *J. Am. Chem. Soc.*, 1959, **81**, 3697-3701.

[6] E. J. Corey, D. E. Cane, *J. Org. Chem.*, 1971, **36**, 3070-3070.

[7] Đ. Škalamera, K. Mlinarić-Majerski, I. Martin Kleiner, M. Kralj, P. Wan, C. Bohne, N. Basarić, *J. Org. Chem.*, 2017, **82**, 6006-6021.

[8] E. Rochlin, Z. Rappoport, *J. Org. Chem.*, 2003, **68**, 216-226.